



From oral formulations to drug-eluting implants: using 3D and 4D printing to develop drug delivery systems and personalized medicine

Niels G. A. Willemen^{1,2} · Margaretha A. J. Morsink^{1,2,3} · Devin Veerman⁴ · Classius F. da Silva⁵ · Juliana C. Cardoso⁶ · Eliana B. Souto^{7,8} · Patrícia Severino^{1,6,9}

Received: 4 February 2021 / Accepted: 21 June 2021 / Published online: 4 September 2021
© Zhejiang University Press 2021

Abstract

Since the start of the Precision Medicine Initiative by the United States of America in 2015, interest in personalized medicine has grown extensively. In short, personalized medicine is a term that describes medical treatment that is tuned to the individual. One possible way to realize personalized medicine is 3D printing. When using materials that can be tuned upon stimulation, 4D printing is established. In recent years, many studies have been exploring a new field that combines 3D and 4D printing with therapeutics. This has resulted in many concepts of pharmaceutical devices and formulations that can be printed and, possibly, tailored to an individual. Moreover, the first 3D printed drug, Spritam®, has already found its way to the clinic. This review gives an overview of various 3D and 4D printing techniques and their applications in the pharmaceutical field as drug delivery systems and personalized medicine.

Niels G. A. Willemen, Margaretha A. J. Morsink, and Devin Veerman have contributed equally to this work.

✉ Eliana B. Souto
ebsouto@ff.uc.pt

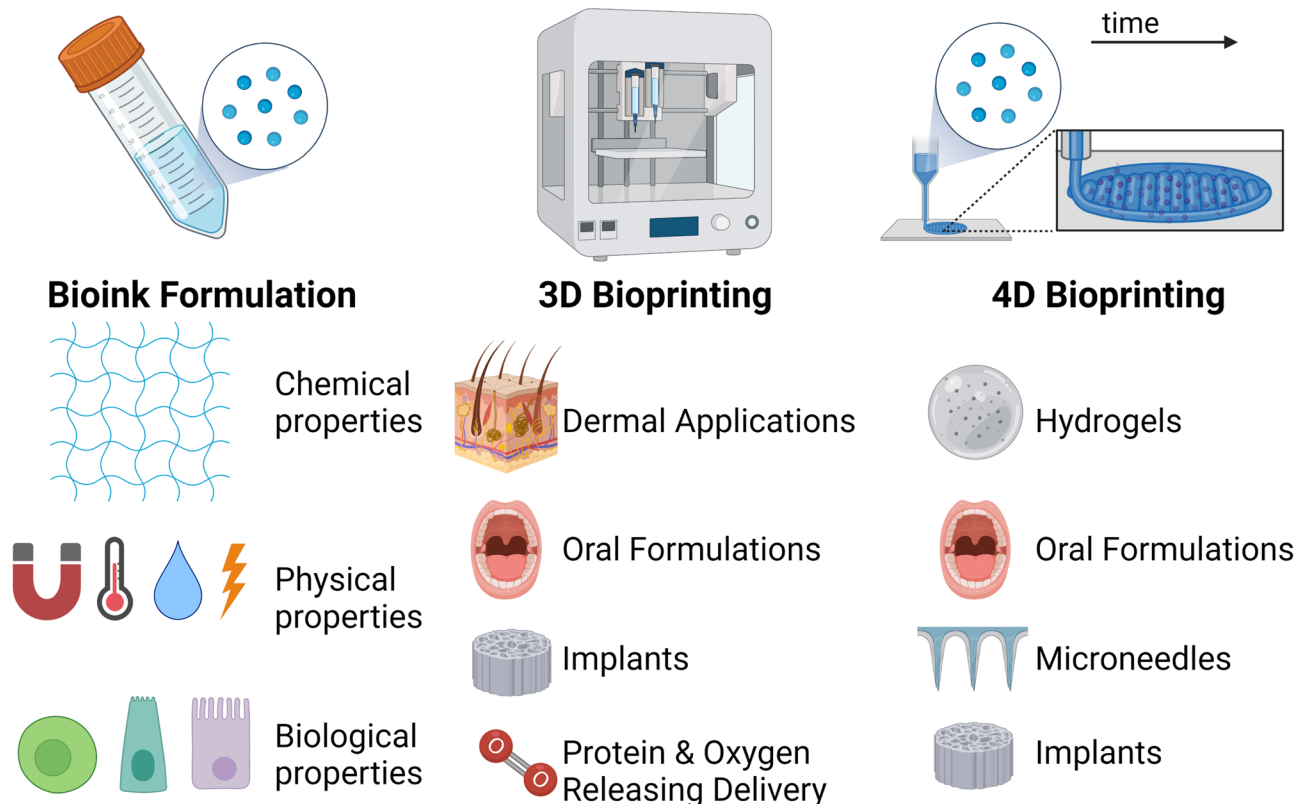
✉ Patrícia Severino
patricia_severino@itp.org.br

- ¹ Center for Biomedical Engineering, Department of Medicine, Brigham and Women & Hospital, Harvard Medical School, 65 Landsdowne Street, MA 02139 Cambridge, USA
- ² Department of Developmental BioEngineering, Faculty of Science and Technology, Technical Medical Centre, University of Twente, Enschede, The Netherlands
- ³ Translational Liver Research, Department of Medical Cell BioPhysics, Technical Medical Centre, Faculty of Science and Technology, University of Twente, Enschede, The Netherlands
- ⁴ Targeted Therapeutics, Department of Biomaterials Science and Technology, Faculty of Science and Technology, University of Twente, Enschede, The Netherlands

- ⁵ Department of Chemical Engineering, Institute of Environmental, Chemical and Pharmaceutical Sciences, Federal University of São Paulo, Rua São Nicolau, 210, Diadema 09913-030, Brazil
- ⁶ University of Tiradentes (Unit), and Institute of Technology and Research (ITP), Av. Murilo Dantas, 300, Aracaju 49010-390, Brazil
- ⁷ Faculty of Pharmacy, University of Coimbra, Pólo das Ciências da Saúde, Azinhaga de Santa Comba, 3000-548 Coimbra, Portugal
- ⁸ CEB - Centre of Biological Engineering, University of Minho, Campus de Gualtar, 4710-057 Braga, Portugal
- ⁹ Tiradentes Institute, 150 Mt Vernon St, Dorchester, MA 02125, USA

Graphic abstract

Bioprinting for Drug Delivery



Keywords Drug delivery systems · 3D/4D printing · Drug-eluting implants · Microneedles · Oral formulations

Introduction

The evolving field of diagnostics has led to some major insights into the mechanisms of certain diseases. One of the areas that has produced important findings is that of individual variations in the effects and progression of disease; these findings have opened the door to developing medicines that can be tuned to an individual, referred to as personalized medicine. In short, personalized medicine takes all the biochemical and physiological aspects of an individual into account when developing therapeutic agents [1].

In 2015, the United States National Institutes of Health set up the Precision Medicine Initiative, which further raised interest in the concept of personalized medicine. An example that perfectly describes the need for personalized medicine is that of child patients receiving cut-up pills and tablets which are meant for adults [2, 3].

However, personalized medicine does come with certain challenges. One major challenge is the production of

these personalized medicines, which raises questions like: How can they be tailored to meet individual needs? How much time does it take to make a personalized therapeutic, and how can they be made routinely?

Here, 3D and 4D printing could aid in the development of personalized medicine. This novel technology was first described by Charles Hull in 1986 and enables printing of three-dimensional objects with different geometries through the deposition of various (bio)materials [4]. When printing with ‘smart materials’, which can change shape and function over time after external stimuli, the process is known as 4D printing [5].

Since 3D printing has become immensely popular in recent years, especially in the field of tissue engineering [6], equipment to utilize this technique has become cheaper and widely available. Furthermore, 3D printing is highly flexible and could be ideal for developing drug-delivery systems which could, in turn, be tailored to personalized medicines. For example, pills and tablets that

contain various therapeutic agents (i.e., polypills) with personalized doses could be printed easily and routinely [7].

When searching for research articles published in the last 10 years using the Web of Science database (Clarivate Analytics), it becomes clear that the pharmaceutical field also can use the 3D printer to its advantage. The first 3D-printed drug, Spritam®, was FDA approved in 2015, which led to an immense leap in the number of articles published [8]. From oral formulations to drug-eluting implants, devices that can be tailored to administer personalized medicine have elicited extensive interest. The trend of published research articles when searching for terms such as ‘3D printing drug delivery’ and ‘4D printing drug delivery’ can be seen in Fig. 1.

Regarding the term ‘3D printing drug delivery’, the exponential increase in the number of articles indicates that papers with this term are still steadily being produced. It is worth noting that although the term ‘4D printing drug delivery’ was mentioned in 26 review papers, only 16 research papers on the topic were published in the last 10 years. Moreover, 12 of the 16 papers were published in the last two years, suggesting that this field is upcoming.

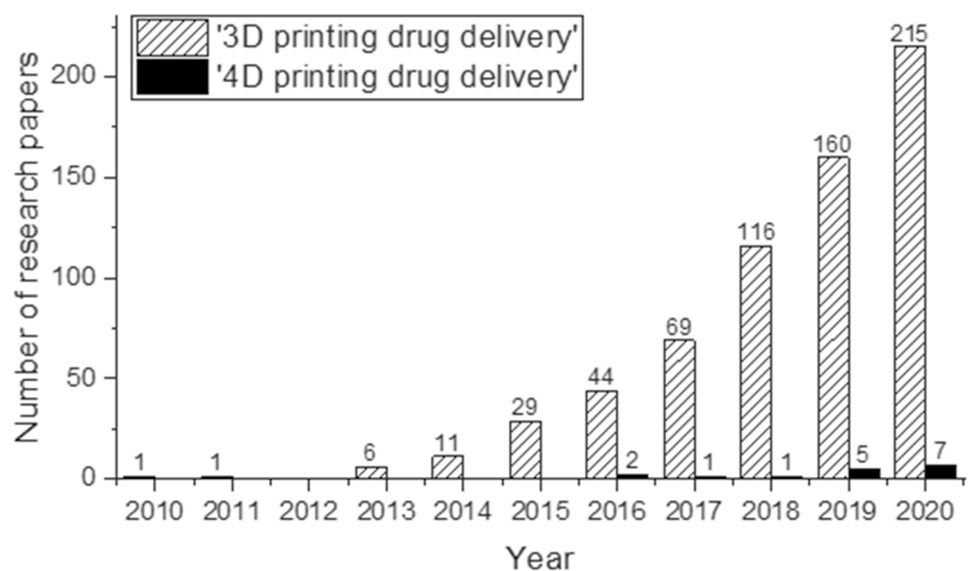
In recent years, many review papers have discussed various techniques and applications of 3D printing in the pharmaceutical field. Interestingly, only a few of these have mentioned 4D printing applications for pharmaceuticals. This emphasizes the need for a comprehensive review paper on the subject. In this review, we provide an overview of the latest conventional and innovative bioprinting technologies, as well as aspects of and prerequisites for formulating bioinks. A comprehensive discussion on 3D bioprinting in drug delivery applications, addressing the wide range of administration routes, is also given. Finally, we thoroughly cover the use of 4D printing to design drug delivery systems,

oral formulations, hydrogels, implants, biomaterials for the release of proteins and oxygen, and customized dosage forms.

Bioprinting technologies

3D bioprinting technologies can be used to mimic tissues, organs, or other biological constructs. There are various techniques for acquiring a desired bioprinted construct, and the bioink plays a large role for both choice of printing technique and in creating a proper construct [9]. The three basic approaches to 3D bioprinting technology are biomimicry, autonomous self-assembly, or mini-tissue building blocks [9, 10]. Biomimicry refers to simulation of a tissue’s biological function and structure and its incorporation in the 3D-printed construct [11]. This can be achieved by choosing the optimal materials to obtain a specific scaffold and stiffness, and specific chemical gradients, as these all affect the proliferation, migration, differentiation, and function of cells [9–12]. Autonomous self-assembly employs embryonic organ development as a model to mimic a tissue, building it up based on early cell types, cell interactions, and extracellular matrix (ECM) formation. 3D-bioprinted constructs using this method manipulate the embryonic pathways [9, 10, 13]. The last approach builds up mini-tissues; in other words, it involves bioprinting of the smallest units of an organ or tissue [9]. The mini-tissues can then be combined to form a larger, more complex construct using a biologically inspired structure. All three of these approaches can be combined to form complex biological tissues. In some cases, the tissue must mature over time, since the tissue is always dynamic. In such cases, 4D bioprinting can offer an alternative. 4D bioprinting adds to 3D bioprinting technologies the 4th dimension (time), which can be achieved in

Fig. 1 Number of publications since 2010 when searching for ‘3D printing drug delivery’ and ‘4D printing drug delivery’. The results were refined to ‘ARTICLES’ in ‘Document Types’. Data was extracted from the Web of Science v.5.35



various ways [14]. Bioinks are especially important here, as they can allow maturation of bioprinted tissue [15]. In this section, we will discuss conventional and novel bioprinting techniques, together with the prerequisites that bioink must meet. Table 1 gives an overview of the bioprinting techniques, including their advantages and limitations.

Conventional bioprinting technologies

Conventional 3D-bioprinting technologies are all nozzle-based techniques, in which bioinks are printed layer by layer according to a spatial control in order to create a specific structure. The methods include inkjet-based, light-assisted, and extrusion-based technologies [10, 18, 32].

Inkjet-based 3D bioprinting

Inkjet-based 3D bioprinting is the most widely used method. It equips a syringe and needle, which carefully deliver the bioink to predetermined locations. Small droplets of bioink from the nozzle are deposited in a spatially controlled manner and crosslinked to form a construct. The advantages of inkjet-based 3D bioprinting include fast printing speed at 1–10,000 droplets/s, ease of use, and low-cost printers [33]. Drop-by-drop printing allows for even distribution of a drug within the bioprinted construct, ideal for drug delivery purposes. However, as there is no continuous flow, it is challenging to print biologically relevant constructs [16, 17].

Extrusion-based 3D bioprinting

Extrusion-based 3D bioprinting works by using pressure or other physical forces to disperse bioink through a microsized nozzle, creating a continuous filament that allows for layer-by-layer bioink deposition [34]. Fused deposition modeling (FDM) can be used with a temperature-controlled extruder to print thermoplastic material into the desired shape [35]. In contrast to inkjet-based printing, extrusion-based 3D bioprinting has a constant flow and can, therefore, print bioinks smoothly onto a substrate [14, 32]. Incorporation of a drug in the bioink is possible prior to printing, allowing for constant drug release through biodegradation. However, extrusion-based printing speed is relatively slow at 10–50 $\mu\text{m/s}$, resulting in decreased viability of larger constructs [21].

Light-assisted 3D bioprinting (stereolithography)

Light-assisted 3D bioprinting, or stereolithography, uses a digital micromirror-array device to control millions of micromirrors in order to crosslink a photo-polymerizable bioink in the desired shape [24]. This method can be used to quickly print various complex biological structures, however only with photocrosslinkable bioinks [25, 26]. The main

Table 1 Advantages and limitations of bioprinting technologies

Technique	Note	Advantages	Limitations	References
Inkjet-based	Conventional	Fast printing speed; very high printing resolution; low cost; possibility for concentration gradient; controlled drug dispersion	Low cell viability; no continuous flow of bioink; requires low viscosity material/liquid material; low cell concentrations	[9, 16, 17]
Extrusion-based or microextrusion	Conventional	Applicability of wide variety of bioinks; continuous flow; possibility for multi-head printing; very high cell densities	Slow printing speed; lower resolution; shear stress on cells	[9, 18–21]
Light-assisted or Stereolithography	Novel multi-material bioprinting	Multiple materials allow for more complex structures	Clogging; low printing speed	[22]
	Novel embedded bioprinting	Fewer geometrical restrictions on the final construct	Slow printing speed; requires a compatible sacrificial bath	[23]
Selective laser sintering	Conventional	Good printing speed and resolution; complex structures possible	Limited to photo-polymerizable bioinks; question-able cytotoxicity	[18, 24–26]
	Novel multi-material bioprinting	Precise structures with complex architectural features	Limited scaling; automation; material selection	[27]
Laser-assisted	Conventional	Allows use of powder materials; relatively fast	Effects chemical stability of natural polymers and drugs	[28, 29]
	Conventional	Nozzle-free system, no clogging; high cell concentration possible; high cell viability	Time-consuming; requires fast-gelling bioink; difficult to accurately position cells/cell constructs; high cost	[18, 30, 31]

advantages are its high printing speed at 200–1600 mm/s, high resolution (depending on the size of the micromirrors), and high cell viability. Additionally, drugs can be mixed with the bioink prior to printing, leading to incorporation within the matrix and controlled drug release. The key limitation is a smaller selection of bioinks which mostly rely on UV-dependent crosslinking, possibly risking carcinogenesis as a result of ROS formation [36].

Selective laser sintering

Selective laser sintering (SLS) employs a laser beam to heat and solidify powder particles, allowing for additive manufacturing of powdered materials. Therefore, the materials used for drug delivery in SLS are the most similar to conventional drug tablets, creating a wide range of opportunities. The advantages of SLS include its high printing speed and use of powdered materials; however, the use of the laser can modify the chemical stability of the biomaterial and drugs [28, 29].

Laser-assisted 3D Bioprinting

The last conventional bioprinting technique is laser-based bioprinting; this technique involves a focusing system, a laser beam, a substrate for the bioink, the bioink itself, and an absorbing layer, and it is nozzle-free. The laser pulse passes to the absorbing layer, which results in evaporation of the material. Subsequently, this creates a high pressure, which causes a stream of bioink towards the substrate onto which the structure can be printed [18]. It is perfect for low-viscosity bioinks, can handle high cell densities, and can achieve very high resolutions, thereby allowing better control of drug placement within the construct. However, the limitations include high cost and high complexity, low-viscosity bioinks resulting in printing of only thin structures, and limits to the polymerization mechanisms of the bioinks [37].

Novel bioprinting technologies

Novel 3D bioprinting technologies aim at overcoming the geometrical limitations of conventional 3D bioprinting by combining it with advanced biomaterials. For example, multi-material 3D bioprinting, which employs an extrusion-based 3D printer, can form intricate structures that replicate biological tissues, using the mini-tissue approach. However, this approach is hampered by clogging and low printing speed [22]. Others have developed a light-assisted 3D multi-material printing approach that yields precise architectural features. The main benefits are minimized mixing of the different bioinks and the large scope for highly precise

structures; however, the drawbacks of this technique are scaling, automation, resolution, and bioink selection [27].

Embedded 3D bioprinting employs a microextrusion printer, which extrudes the desired pattern into a sacrificial printing bath. The sacrificial bath is removed after crosslinking the desired printed construct. This allows for fewer geometrical restrictions on the final construct. The main limitations of this technique are low printing speed and the requirement for a compatible sacrificial printing bath [23].

4D bioprinting

4D bioprinting is a novel bioprinting technique which incorporates ‘time’ as the 4th dimension [15]. Through development of a complex bioink, the material can ‘mature’ over time, which overcomes the obstacle of the static nature of 3D bioprinting. Thus, 4D printing can be described as printing with ‘smart’ materials which can change shape and/or function over time after external stimulus. There is increasing interest in this novel approach to mimicking tissues, as the dynamic component can improve the functionality of printed tissues [38–41]. Moreover, it can provide a solution to creating functional vasculature in tissue-engineered constructs, with printed channels and incorporated vascular growth factors [15]. This can be achieved using either responsive materials or the bioprinted construct’s maturation through cellular coating or self-organization [15]. The responsive bioink reacts to external stimuli, such as temperature, humidity, pH, ions, or acoustic, electrical, or magnetic fields, which results in morphological changes [15, 42–44]. Cell maturation within 4D bioprinted constructs can be realized with cell coatings, with self-organization based on cell location or cellular spheroids, or by using matrix deposition [15]. The printing approach used for 4D bioprinting may incorporate all the techniques mentioned above.

Stereolithography-based methods for 4D bioprinting have shown potential and require a photocrosslinkable material which can change in shape based on the stimulus [42]. The greatest benefit of 4D bioprinting is that it enables structural changes to a construct over time, resulting in improved applicability. Additionally, opportunities for personalized medicine are created using this technique. The main drawback is the complex design of the bioink, as the effect of stimuli can be detrimental to cell viability [15, 42, 43]. Moreover, the reactions of the immune system remain unknown; therefore in vitro and in vivo testing will be required before clinical translation [45]. Unfortunately, 4D bioprinting is expensive due to high bioprinter and bioink costs, which presents a serious obstacle to this promising technique [46]. The most essential factor of 4D bioprinting is the bioink, which allows for stimuli-responsive mechanisms or for cell maturation; therefore, in the next section, we consider bioink formulation and prerequisites.

Bioink formulations and prerequisites

Bioink formulation is of the utmost importance for 3D and 4D bioprinting, as it can determine the printability and feasibility of a construct. Bioinks are composed of biomaterials and can contain cellular components; thus, the biomaterial poses as the ECM [32, 47]. The biomaterial can be naturally derived or synthetic [48]; a complete overview of biomaterials used for bioinks goes beyond the scope of this review. The reader is referred to the review written by Gungor-Ozkerim et al. [47].

Biocompatibility ensures viability, proliferation, maturation, and other essential cell functions. It is the most crucial parameter of bioink development. An important way in which bioinks can affect constructs is by causing the construct degradation rate to mimic the tissue remodeling and regeneration rate so that the construct is gradually and completely degraded as the tissue is remodeled. Elasticity and viscosity are critical rheological parameters in bioink design, both for the final construct and for printability. Elasticity heavily influences cellular behavior, including cell attachment and proliferation, through mechano-transduction cell signaling. In addition, the water absorption is altered, which is an essential parameter for nutrition flow. If the ink is too viscous for printability, it can clog the nozzle and impede the printing process. Shear stress and yield stress are also important for cell survival and distribution [32]. Physical or chemical crosslinking mechanisms can be employed to maintain the construct's stability over time [48]. Other chemical aspects of bioink include possible chemical modification of the biomaterial by adding biochemical motifs such as RGD sequences, to which cells readily adhere [49].

Lastly, biological considerations include cell type and structure viability. Different cell types have different reactions with biomaterials and bioprinting processes, which should be carefully evaluated. Cells can be printed as single cells or cell aggregates, such as spheroids, to obtain a desired engineered tissue. Single cells are more easily printable, as the corresponding preparation of the bioink is less complicated and results in higher cell viability [48, 50]. Moreover, the biological component of a bioink can improve tissue maturation via the addition of growth factors, chemokines, cytokines, and other compounds to promote angiogenesis and cell differentiation [49]. The prerequisites for bioinks and stimuli-responsive techniques that can be used for 4D bioprinting are summarized in Fig. 2. The use of materials that can alter shape upon different stimuli, for instance, moves a technique into the fourth dimension. Therefore, 4D bioprinting is becoming increasingly important for drug delivery applications.

3D-bioprinting drug delivery applications

3D-printed dermal applications for drug delivery

Transdermal medications have existed for many years, and have several advantages; they are easy to use, non-invasive, pain-free, and ideal for self-administration. However, the stratum corneum's impermeability makes penetration of drug molecules across the skin difficult without injections [51]. Thus, fabrication of high-resolution microneedle patches, with sizes ranging from 150 to 200 microns, has become a trending research topic since the mid-1990s. Nowadays, researchers use many 3D printing techniques to print entire microneedle patches or alternatively, coat printed patches with the desired drug solution.

The use of two-photon polymerization (TPP) to fabricate hollow microneedles attached to a drug reservoir for transdermal delivery of drugs has gained more interest over the last few years [52, 53]. Moussi et al. used TPP to print hollow microneedles connected to a reservoir that can load and extract fluids at flow rates ranging from 20 to 160 $\mu\text{L/s}$. They managed to retain a high resolution, but this was linked to relatively small constructs (only 0.3 to 3 mm^3). They also assessed the microneedles' delivery capabilities on polydimethylsiloxane (PDMS) and mouse skin and showed 100- to 180- μm -deep fluorescent dye delivery into the skin. Moreover, subsequent cell culture studies showed excellent cytocompatibility of the microneedle arrays [52].

The use of inkjet bioprinting to build complex 3D structures has not been extensively explored and this method has mostly been used to create two-dimensional patterns. For example, Ross et al. coated metallic microneedle arrays with multiple insulin-containing polymer layers for transdermal insulin delivery [54]. In another study, a similar approach was followed to coat metallic microneedles with layers of a copolymer containing 5-fluorouracil (5-FU), curcumin, and cisplatin as drugs. The results showed significantly increased release profiles of the drugs in porcine skin when coated onto the microneedles [55].

Yin et al. made a drug-encapsulated microneedle patch system with an integrated 3D-printed microheater device [56]. Applying heat can accelerate drug diffusion and aid in the controlled delivery of drugs [57], and may be an interesting addition to already established microneedle patches to enhance transdermal drug delivery and create a smart-sensor-assisted microneedle patch [56]. The microheater device was printed using a Cellink 3D bioprinter. The device was composed of multiwalled carbon nanotubes (MWCNTs) and PDMS and could reach temperatures up to 44 $^{\circ}\text{C}$. The presence of PDMS enabled tuning of the interfacial tension, allowing the microheater unit to

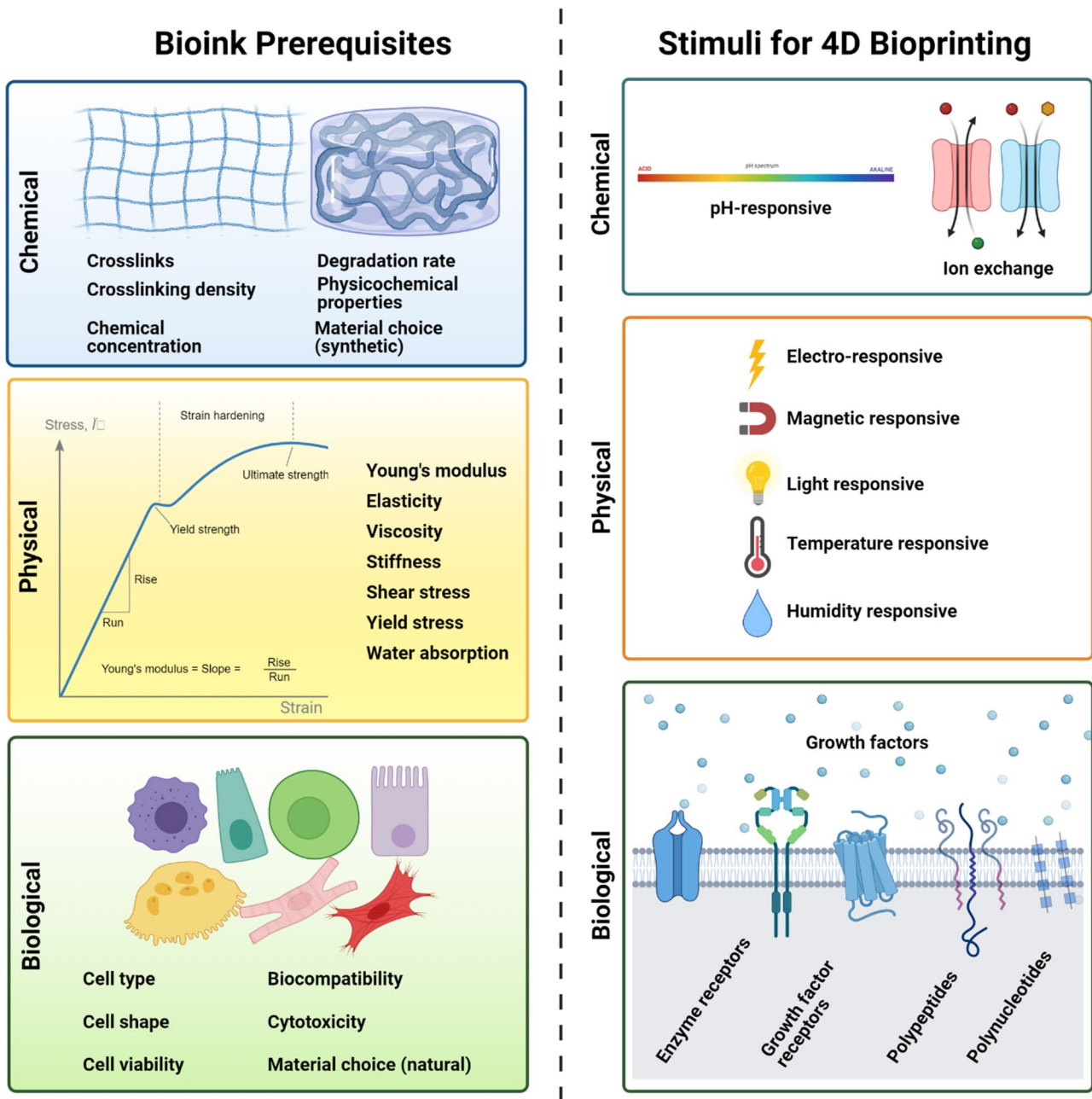


Fig. 2 Summary of prerequisites for bioink formulations and stimuli for 4D bioprinting, categorized per chemical, physical, and biological properties

be printed on multiple substrates, including paper, a latex glove, and a microneedle patch (Fig. 3a). The researchers assessed the microheater's functional ability in vitro on rat skin and showed increased release and diffusion of Cy5 [56].

Pere et al. used stereolithography with a UV photopolymerization step to 3D print a pyramid and cone microneedles for insulin delivery. A solution of insulin, xylitol, mannitol, and trehalose was printed onto a microneedle surface using a piezoelectric-based inkjet printer. The in vitro release

studies on porcine skin showed a 90–95% release within 30 min [58].

In another study, Luzuriaga et al. also applied fused deposition modeling to print polylactic acid-based biodegradable microneedles with fluorescein. Since printing resolution is a major limitation with fused deposition modeling, the authors researched several microneedles parameters, such as the length, shape, and array density, and showed these can easily be tuned with 3D printing and chemical etching methods [59].

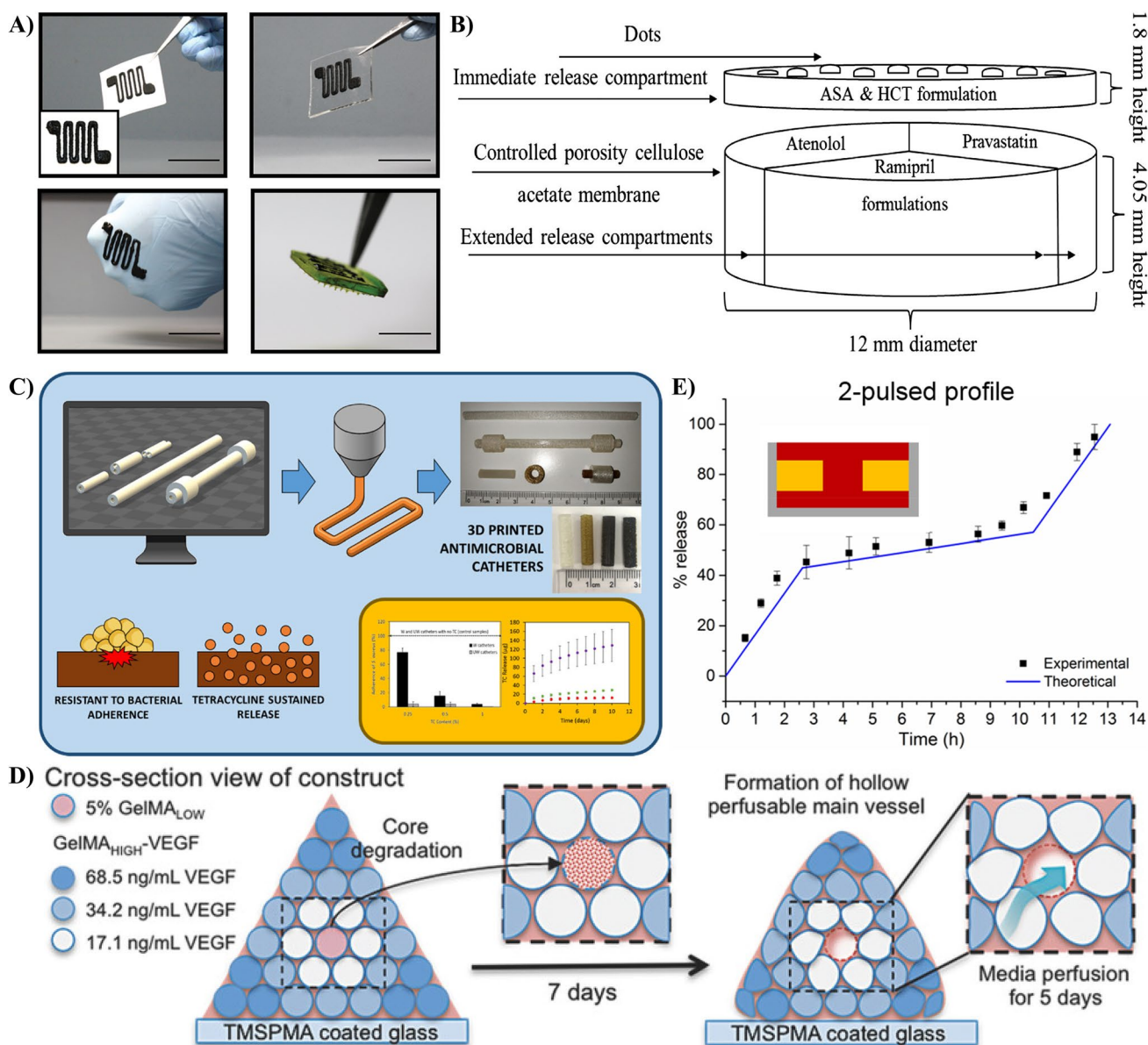


Fig. 3 Various 3D bioprinting applications. **a** 3D printing of a micro-heater onto Printed paper (upper left), PDMS (upper right), experimental glove (lower left), and surface of a cellulose microneedle patch (lower right). Reproduced with permission from [56], Copyright 2019, John Wiley & Sons. **b** Schematic of a polypill design with a hydrochlorothiazide and aspirin immediate-release compartment, and a pravastatin, atenolol, and ramipril sustained-release compartment. Reproduced with permission from [60], Copyright 2015, Elsevier. **c** Illustration of the 3D-printed antimicrobial catheter produced

with fused deposition modeling. Reproduced with permission from [61], Copyright 2019, American Chemical Society. **d** 3D bioprinting of a perfusable lumen lined with HUVECs within a pyramidal construct using a VEGF-functionalized GelMA bioink. Reproduced with permission from [95], Copyright 2017, John Wiley & Sons. **e** Customized release of two drugs at the same time with constant release of phenylephrine HCL and two-pulsed release of diphenhydramine HCL. Reproduced with permission from [103], Copyright 2020, Elsevier

3D bioprinting has also been introduced in wound healing because it enables complex micro-architectures with cellular material [63–68]. Long et al. recently developed an extrusion-based 3D-printed chitosan-pectin wound dressing loaded with lidocaine, a common anesthetic drug [66]. The construct showed extensive swelling, with increased water absorption properties, dimensional integrity, excellent

printability, and self-adhesion to the skin, all favorable properties suited to a moist wound environment. In another study, Maver et al. 3D printed several drug-loaded alginate dressings for wound healing. The in vitro assessments showed an immediate onset of action when lidocaine was incorporated, but extended release profiles up to 2 days were observed for diclofenac sodium-loaded dressings [68]. Muwaffak et al.

used 3D printing to prepare antimicrobial-loaded polycaprolactone wound dressings (with silver, zinc, and copper as antimicrobials) in the shape of a nose and an ear. Despite the limitations in 3D printing resolution, they managed to print filaments with relatively low deviations in diameter. They showed dual releases of the metals, with initial fast release over 24 h and slower release over 48 h, thereby minimizing the necessity of frequent medical intervention. 3D-printed masks specific for patients have great potential for personalized wound dressings for chronic wounds [69].

3D-printed oral-drug-releasing formulations

3D printing allows for much more manufacturing flexibility than traditional methods for producing tablet medicines [70]. Its capacity to make complex tablets with immediate release, extended release, delayed release, pulsatory release, and incorporate multiple drugs and multiple release profiles all in one tablet, has opened more possibilities than simple tablet compression [71]. For example, Sadia et al. recently showcased a novel tablet design of a tablet that increased immediate drug release of 3D-printed tablets. The tablets, made from polymethacrylate, contain built-in channels of controlled width, length, and configuration. These channels increase the tablet's surface-area-to-volume ratio, thereby facilitating faster immediate drug release. However, the use of fused deposition modeling as the 3D printing technique affected the resolution of the channels. Higher resolution would increase the complexity of the printed construct as well as the drug loading capacity, potentially aiding in more controlled release of the drug [72]. In another study, Khaled et al. also showed the relationship between surface area and drug release, with tablets of higher surface-area-to-volume ratios having faster drug release. Moreover, they were able to use a high drug load of paracetamol (80%) without changing the printing ink's chemical or physical properties. Again, resolution of the printed construct was low, owing to the limitations of the extrusion-based 3D printing technique [73].

Khaled et al. formulated a polypill which contained up to five different drug doses (aspirin, hydrochlorothiazide, atenolol, ramipril, and pravastatin) in separate compartments (Fig. 3b). They controlled drug release independently with different release membranes and matrices [60]. However, the combination of more than one drug in the same tablet could result in larger tablets, which can be harder for patients to take. In another study, Li et al. combined hot extrusion melting with fused deposition modeling to create a double-chamber drug delivery device for diabetic treatment. A dual-nozzle 3D printer was used to formulate a device where a tablet was embedded within a larger tablet (DuoTablet) in a single process. Each tablet contained different glipizide dosages, thereby offering both fast and delayed drug release for a sustained-release

profile. The authors did indicate that they observed reduced drug loading efficiency (under 5% drug loading) owing to the limited mixing ability and high shear force of the extruder at high drug-loading percentages [74].

Kadry et al. used an FDM printer to create tablets with various infill densities and patterns, favorable for multi-drug printing as they allow more control over the release profile. The *in vivo* oral absorption of a diltiazem-loaded hydroxypropyl methylcellulose tablet was closely correlated to oral absorption results from *in vitro* studies. Moreover, they showed that tablets with a hexagonal infill dissolved faster than those with infills of other shapes [75].

Tablet-in-device systems, which retain printed tablets within a gastric floating system, help increase the gastric retention time of tablets, which is essential for sustained release of the contained drugs. For example, Li et al. studied the effect of infill rate and percentage on the buoyancy and drug release rate of gastro-floating tablets. They used hydroxypropyl methylcellulose for hydrophilic matrices and microcrystalline cellulose as the molding agent. The study showed that as the lattice density increased, the tablet weight increased, forcing it to sink and increasing drug release rates. They also formulated tablets with floating times of over 8 h [76]. In a recent study, Linares et al. developed a pH-sensitive tablet to release a drug specifically in the colon. They used a combination of fused deposition modeling and injection volume filling to simplify the incorporation of drugs into a scaffold at room temperature. This enabled the authors to print at higher temperatures and higher drug-loading percentages compared to regular fused deposition modeling. In addition, the enteric film coating the tablets, made from hydroxypropyl methyl cellulose (HPMC) gel and Eudragit FS30D, was pH-sensitive, and tailored dissolve at colonic physiological pH. At low pH (1.2), the tablet released only 2.3% of the drug, while at high pH (7.5), it released over 80% of the drug in 8 h. Although the drug load was limited to only 0.36%, the tablets successfully showed a delayed profile that released the drug only in the colon [77].

A different oral formulation, in the shape of a mouthguard, was developed by Liang et al. They formulated a drug-releasing mouthguard that can be specifically tailored to the patient's anatomical features. The mouth guards were produced by FDM and based on intraoral scans of the patient. They used PLA and PVA loaded with clobetasol propionate and vanillic acid, both released in a controlled manner. The *in vivo* human studies showed that these mouthguards displayed similar release kinetics over three cycles of wear. However, the mouthguards also exhibited faster drug release kinetics than their *in vitro* counterparts, probably due to tongue movement and intense salivation [78].

3D-printed drug-eluting implants

Biomedical implants are typically placed inside the body to replace a missing body tissue or recover its function, thereby significantly improving the patient's quality of life. However, nowadays, the implant field has moved towards personalization and customization, leading to site-selective and controlled drug-releasing implants. The complex design and requirements of these implants are difficult to attain with conventional manufacturing techniques. Thus, over the last decade, 3D printing has been utilized to fabricate implantable drug delivery systems which can be highly valuable in modern medicine. One proof of this is that clinicians increasingly favor the local release of chemotherapeutic agents, resulting in lower systemic blood drug concentration, fewer adverse effects, and increased antitumor efficacy [79, 80]. Thus, more research has focused on 3D printing of biodegradable and drug-releasing implants to increase chemotherapeutic efficiency. Wang et al. prepared biodegradable poly L-lactic acid (PLLA)-based drug-loaded implants. When implanted into test animals, they showed high local drug concentrations, resulting in increased local antitumor efficacy and reduced systemic side effects [81]. In another recent study, Yang et al. 3D printed biocompatible and biodegradable poly-lactic-co-glycolic acid (PLGA) implants loaded with 5-FU and NVP-BE235 (both antitumor agents) using electro-hydrodynamic jet (E-jet) printing. When implanted in a mouse model, the implants inhibited breast cancer growth and reduced distant metastasis. Moreover, compared to systemic injections, the implants significantly reduced the drug dosage needed for effective treatment [82].

The choice of the polymeric matrix also has a significant effect on drug release kinetics. For example, Bose et al. studied release of curcumin, a natural compound with medicinal properties [83], from PLGA-PEG and PCL-PEG polymers onto hydroxyapatite. They used a light-assisted printing technique and were able to print constructs at high resolution and printing speeds. The results showed increased cell viability and curcumin release from the PCL-PEG composite. Moreover, the group coated 3D printed tricalcium phosphate with curcumin-PCL-PEG and showed increased mineralized bone formation after six weeks of *in vivo* implantation [84]. Coating the surface of 3D-printed implants is a standard method to improve their overall biocompatibility. Dydak et al. 3D printed Ti6Al7Nb implants using selective laser melting and subsequently coated the surface with gentamicin, a common antibiotic. The release of gentamicin from the coating significantly increased the implant's antibiotic properties, thereby potentially accelerating the recovery process and decreasing the risk of infection [85].

Hosseinzadeh et al. developed a drug-eluting 3D-printed hydrogel-based mesh for the treatment of glioblastoma

(GBM) [86]. The mesh, which was referred to as GlioMesh, was loaded with PLGA microspheres containing temozolomide (TMZ), a chemotherapeutic drug. A microextrusion 3D bioprinter was used to fabricate the drug-eluting mesh, utilizing a mixture of the microspheres, alginate, and calcium chloride to cross-link the structure. The resolution of the GlioMesh was limited because incorporation of the TMZ-loaded microspheres reduced the viscosity of the ink. To prevent clogging of the nozzle, the amount of microspheres loaded into the mesh was limited to a maximum of 14 mg/mL. The paper did not mention whether the limited loading capacity could eventually hamper *in vivo* application. However, *in vitro* release studies at 37 °C showed that GlioMesh induced sustained release of TMZ over 56 days, versus 16 to 20 days for TMZ-microspheres, which highlights the benefit of using a drug-eluting hydrogel mesh. Experiments using human GBM cell lines U251 and U87 MG demonstrated the same sustained release period. Moreover, GlioMesh had superior cytotoxic effects over free TMZ. The group argued that the latter is due to the drug's slow degradation, which maintained autophagy in the human GBM cell lines. It is also noteworthy that GlioMesh induced a higher degree of mitochondrial damage compared to free TMZ. Overall, this study, conducted by Hosseinzadeh et al., demonstrated using a biocompatible and biodegradable drug-eluting alginate-based mesh to facilitate a sustained release of TMZ with great potential [86].

Other medical implants such as catheters and stents are generally coated with an active solution [62], but 3D printing offers better spatial control in the fabrication process and increased drug-loading efficiency. Recently, Mathew et al. used fused deposition modeling to produce tetracycline hydrochloride-loaded polyurethane catheters to prevent bacterial colonization (Fig. 3c). They showed increased antibacterial effects for up to 10 days and a 99.97% reduction of bacterial adherence. However, as indicated by the authors, the surface roughness of the printed constructs (a limitation from using fused deposition modeling) might be problematic when used in patients. Nonetheless, the authors showed the potential of using 3D printing to manufacture anti-infective catheters [61]. In another study, Weisman et al. developed a gentamicin sulfate and methotrexate-loaded 3D-printed poly-lactic acid catheter. Both of the drugs were successfully dispersed inside the PLA matrix, and they exhibited sustained-release profiles of up to 5 days. Moreover, the gentamicin significantly inhibited bacterial growth onto the catheter [87].

3D-printed protein- and oxygen-releasing biomaterials

Tissue hypoxia is an inevitable problem in tissue defects (e.g., bone fractures) or post-implantation for many reasons,

including lack of vascularization or slow anastomosis (e.g., vascular penetration of only 3 mm in 2 weeks) [88]. A lack of oxygen can eventually lead to lower medical treatment efficiency, increased inflammation and infection, and tissue necrosis [89]. Thus, developing oxygen-releasing biomaterials has become a significant field of interest over the last few years [90–92]. For example, Touri et al. 3D printed scaffolds containing 60% hydroxyapatite (HA) and 40% beta-tricalcium phosphate (β -TCP). After sintering, the scaffolds were dip-coated with a calcium peroxide (CPO)—polycaprolactone (PCL) composite for in situ oxygen production at the implanted site. Their results showed sustained oxygen release, which subsequently promoted bone ingrowth with improved osteoblast cell viability and proliferation under hypoxic conditions [92]. In a later study, they also showed the scaffold's antibacterial properties, with enhanced inhibitory effects against *Escherichia coli* (*E. coli*) and *Staphylococcus aureus* (*S. aureus*) [91].

Incorporating growth factors to stimulate tissue regeneration of implants in vivo (e.g., bone fracture healing or stimulation of vascularization) has also been an important topic of interest [93–98]. Poldervaart et al. encapsulated vascular endothelial growth factor (VEGF) into gelatin microparticles to prolong VEGF release in predefined regions of 3D human endothelial progenitor cell-Matrigel™/alginate constructs. Their 3D bioprinting technique resulted in high viability, also owing to the cytocompatible crosslinking mechanism of alginate and calcium. However, the printed constructs (10 mm \times 10 mm \times 3 mm) were still too small to be clinically relevant. In vivo analysis showed temporal and controlled release of VEGF, which significantly increased vessel formation [97].

Byambaa et al. 3D printed a cell-loaded vascularized bone construct with vasculogenic and osteogenic regions (Fig. 3d). Since they printed the rods individually, they were able to attain precise control over the spatial composition despite using extrusion-based printing techniques. However, individually printing the rods did affect the printing speed. The construct consisted of a central perfusable vascular lumen with bioactive VEGF-conjugated-COOH gelatin methacryloyl (GelMA), containing human umbilical vein endothelial cells (HUVEC) and mesenchymal stem cells (MSC). This was surrounded by silicate nanoplatelet-loaded GelMA cylinders, which induced osteogenic differentiation of MSCs [95].

Another study performed by Chen et al. incorporated two growth factors, BMP-2 and VEGF, into a hydroxyapatite/gelatin/chitosan composite to stimulate osteogenesis and angiogenesis, respectively. Previous studies on repairing bone defects by implanting scaffolds limited rat defect sizes to 5 mm in diameter. The researchers tried to repair 15-mm defects in a rabbit model. They observed that the scaffolds degraded gradually and were replaced by new vascularized

bone, noting more bone formation after 12 weeks compared to the control [96].

3D-printed constructs for personalized drug dosing

3D printing can offer personalized medication, which has stricter requirements for release profiles and complex geometries. It has already been utilized to tailor the shape, dosage, size, and even color of medications. Moreover, it has been applied in multiple forms, including tablets, vaginal rings, and microneedle arrays [99–108]. Thus, 3D printing offers more flexibility for treatments to completely fit the needs of the patient. Table 2 lists examples of constructs obtained by 3D printing techniques for the delivery of different drugs.

Scoutaris et al. developed 3D-printed chewable candy-like formulations (based on Starmix® sweets) to increase the medications' palatability, and thus, pediatric patients' compliance. They could print the tablets in several shapes, including hearts, bottles, lions, and bears, and achieved improved taste (reduced bitterness). Moreover, drug-release studies showed drug dissolution within 60 min of intake [105].

3D printing has also been used to specifically tailor drug-releasing scaffolds to the patient [69, 104]. Goyanes et al. generated a 3D model of a patient's nose with a 3D scanner. Fused deposition modeling and standard lithography were subsequently used to 3D print a salicylic acid-loaded nose-shaped mask to treat acne vulgaris. They found that standard lithography provided higher resolution and drug loading than fused deposition modeling [104].

Fu et al. developed 3D printed progesterone-loaded PLA7pcl vaginal rings of various shapes and dosages using fused deposition modeling. They showed a controlled release of progesterone for more than seven days. Although this technology is far from mature, it offers personalization of shape and dosage, which is still lacking in the progesterone vaginal ring market [99].

Microneedle arrays may also be used for personalized medicine. Lim et al. fabricated a 3D-printed microneedle multifunctional device to treat trigger finger while simultaneously splinting the affected finger. They showed increased penetration of the drug (diclofenac) and outstanding biocompatibility with human dermal cell lines [101].

Sun et al. formulated a customizable drug tablet consisting of three components: (i) a degradable matrix containing the drug, (ii) a non-degradable matrix not containing the drug, and (iii) an impenetrable and biodegradable coating that protects the drug tablet. However, one side of the coating remains permeable, and thus the drug tablet can degrade in a controlled manner (in five release pulses). Potentially, this method can fabricate any drug release profile, depending on the desired release rate. However, the material used is not suitable for human consumption [102]. The authors recently published a

Table 2 Examples of constructs developed by several 3D printing techniques for the delivery of different drugs

Type of construct	3D printing technique	Incorporated drug(s)	Findings	References
Microneedles	Inkjet bioprinting	5-FU, curcumin, and cisplatin	Increased release profiles in porcine skin in vitro	[55]
Microneedles	Stereolithography	Insulin	Increased (up to 90–95%) release of insulin within 30 min on porcine skin in vitro	[58]
Wound dressing films	FDM	Silver, zinc, and copper	Dual release of the metals over 48 h; In vitro antimicrobial activity	[69]
Polypill tablet	3D extrusion printing	Aspirin, hydrochlorothiazide, atenolol, ramipril, and pravastatin	Independent control over drug release; Sustained and immediate drug release; 3D printing did not change the physical form of drugs	[73]
Tablets	FDM	Diltiazem	Adsorption in vivo closely correlated to in vitro adsorption; Shape of tablet influences infill dissolution rate	[75]
Mouthguards	FDM	Clobetasol propionate and vanillic acid	Personalized mouthguards; Similar in vivo release profiles over multiple wearing cycles; In vivo release faster than in vitro	[78]
Implant	E-jet	5-FU and NVP-BEZ235	Inhibition of breast cancer growth; Reduced metastasis; Reduced drug dosages for effective treatment	[82]
Implant	Stereolithography	Doxorubicin, ifosfamide, methotrexate, and cisplatin	High local anticancer drug concentrations with increased antitumor effect; Lower systemic side effects	[81]
Catheter	FDM	Tetracycline hydrochloride	Increased antibacterial effects up to 10 days, 99.97% reduction of bacterial adherence	[61]
O ₂ releasing implant	Robocasting	CPO	Sustained oxygen release which promoted bone ingrowth, cell viability, and cell proliferation under hypoxic conditions	[92]
VEGF-releasing implant	Extrusion-based direct writing	VEGF and silicate nanoplatelets	Formation of the blood vessel with sprouting by HUVEC and MSC migration; Increased osteogenic differentiation of MSC	[95]
Chewable ‘sweets’	FDM and HME	Indomethacin	Reduction in bitterness; Ability to print multiple shapes; Drug dissolution within 60 min of intake	[105]
Vaginal ring	FDM	Progesterone	Controlled release over 7 days; Ability to print multiple shapes and dosage forms, tailored to the patient	[99]

new study on a similar drug tablet designed for the mass population to address this. In this research, they only considered FDA-approved materials to develop their tablets. The tablet is similar to the one in their previous study, also consisting of several parts: (i) an eroding surface matrix containing low amounts of the drug, (ii) an eroding surface matrix containing high doses of the drug, (iii) an eroding surface matrix not containing any drugs and (iv) a coating made of white wax. With this method, they were able to customize the duration

of release, release profile, and dosage, while also combining multiple drugs into one tablet (Fig. 3e) [103].

4D printing applications for drug delivery

In biomedical research, many studies report the application of 4D printing for tissue and organ engineering. This is referred to as 4D bioprinting, and it includes, for example,

the printing of cell-laden structures, self-folding tubes, and biosensors [39–41, 43]. 4D printing of drug delivery systems is something that is rather new, and although some researchers did not mention 4D printing in particular, there were some 4D-printing aspects to their concepts. Since the concept of 4D printing is already explained in Bioprinting Technologies, this section will cover what can be regarded as 4D printing in the field of drug delivery and its main applications.

4D-printed hydrogels as drug-delivery systems

The first application that is worth mentioning is hydrogels. These are made from natural or synthetic polymers and have the unique property of absorbing and retaining large quantities of aqueous material. Furthermore, due to their biodegradability and biocompatibility, hydrogels have found a role as drug delivery systems [109].

Regarding the fourth dimension of hydrogels, the stimuli-responsiveness of certain hydrogels makes them excellent candidates for 4D drug-delivery systems and could aid in the controlled release of drugs [109]. Many studies have shown different techniques with different bioink formulations to realize 4D printing of hydrogels. However, only a few have demonstrated their application as 4D-printed drug-delivery systems.

A 4D hydrogel that acts as a drug-delivery system has been described by Larush et al. [110]. Using a stereolithography (SLA) system with a digital mirror device and a UV-LED light source (ex. 385 nm), Larush and colleagues produced hydrogel tablets with complex structures. These hydrogel tablets were printed from a mixture of acrylic acid and polyethylene glycol diacrylate (PEGDA). The tablets were supplemented with sulforhodamine B, a pH-independent fluorescent dye, as a drug model for small hydrophilic molecules. The group showed that they could control drug release by changing the pH and designing specific geometries with desired surface areas, without inducing cytotoxicity during *in vitro* studies on Caco2-cells [110]. As stated by the group, advancing this technology could potentially lead to personalized medicine, in which the release of certain pharmaceutical agents can be tuned per patient by changing the geometry of the printed tablet. Furthermore, altered drug release upon a change of pH can result in controlled release in specific parts of the body. However, with a current printing duration of 20–40 min per printed structure, speed should be optimized to produce the hydrogel tablets on a larger scale.

Dai et al. used a nozzle-based 3D printer (Envisiontec, Germany) supplemented with a UV-LED (ex. 365 nm) for curing. The created NIR-responsive shape-memory hydrogel consisted of a mixture of pluronic F127 diacrylate macromer (F127DA), poly(lactide-co-glycolide) (PLGA) and graphene

oxide (GO), both of which convert NIR radiation to thermal energy (Fig. 4). Consequently, minocycline hydrochloride, a broad-spectrum antibacterial tetracycline antibiotic, was loaded into the F127DA/PLGA/GO hydrogel. The hydrogel showed shape recovery at temperatures less than 37 °C and mechanical toughness of more than 3.45 MPa in the swollen state, indicating that this F127/DA/PLGA/GO hydrogel has a higher mechanical strength and fatigue resistance than conventional hydrogels. Using NIR light, the hydrogel's shape was altered, which changed the drug release profile of minocycline hydrochloride. This indicates that the group could control drug release from the hydrogel. Furthermore, no cytotoxicity was observed when performing experiments on 3T3 cells. Interestingly, the group mentioned a possible application in the dental field in the form of a personalized drug-eluting temporary crown. However, the printed concept showed a lower elastic modulus than current temporary crowns, which might cause problems even if biting forces are suggested to be kept low after the surgical procedure. Furthermore, although the authors state that the original shape was recovered with only a little residue after stimulating the construct for 5 min using NIR light, this small amount of residue or the temporary shape could potentially reduce the fit of the temporary crown that was initially designed and printed for an individual. Notably, the group is currently optimizing and testing the printed hydrogel *in vitro* and *in vivo*, and will evaluate it in their next work [111].

Wang et al. also studied the concept of shape-memory hydrogels. Here, the group 3D-printed different mixtures of F127DA and alginate using a nozzle-based 3D printer from Envisiontec. UV light (ex. 365 nm) was used to fix the shape. The 3D-printed hydrogel showed higher resolution as compared to a traditional UV-fixed construct. Thereafter, Wang et al. decided to load the hydrogel with the anti-tumor drug methotrexate (MTX), a hydrophobic drug. The MTX was first dissolved in 1-vinyl-2-pyrrolidone (VP) to facilitate drug loading into the hydrogel. Results showed that the gel folded upon external stress and, when the stress was released, recovered after 30 min. Unfortunately, the group did not find shape recovery of the printed construct at 37 °C, nor recovery without fixing and defixing the temporary (i.e., folded) shape using chemicals. Regarding drug release from the printed construct, results showed that the drug release profile was altered when the construct was in the temporary state. The gel demonstrated excellent cell viability on 3T3 cells, and *in vitro* degradation experiments showed sufficient biocompatibility [79].

More recently, Jiang et al. used a nozzle-based 3D printer (3D Bioprinter V2.0, China) to create a glycerol-modified PVA hydrogel reinforced by a 3D-printed PCL-graphene scaffold, referred to as PG-Pg. The hydrogel was supplemented with sodium fluorescein as a model drug. The hybrid PG-Pg hydrogel showed low friction, high water retention,

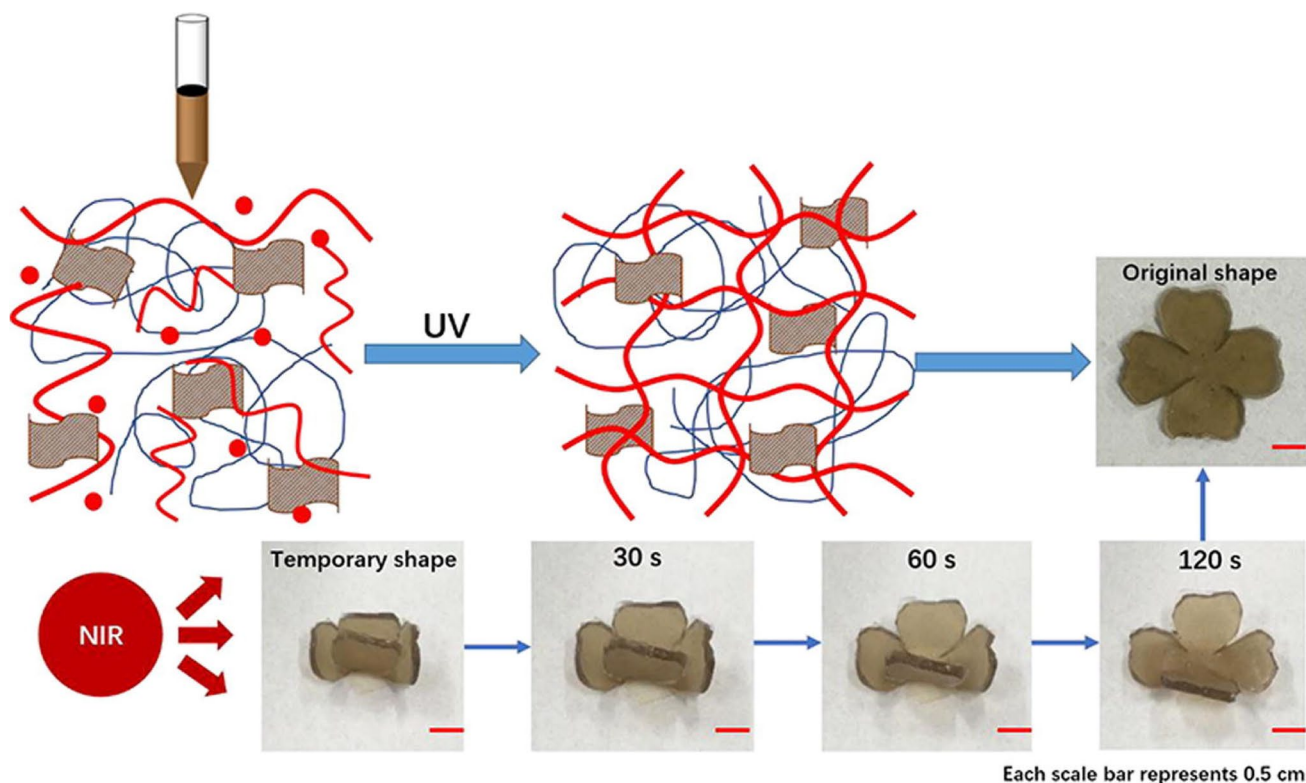


Fig. 4 4D-printed shape-memory hydrogel F127DA/GO produced by Dai et al. The gel is cured by using UV light, and upon NIR stimulation, the printed shape is altered and returns to the initial shape after

less than 5 min. Reproduced with permission from [111], Copyright 2018, Elsevier

excellent stiffness, and toughness. In addition, the PG-Pg hydrogel showed low protein and cell absorption, indicating its potential for *in vivo* applications. More specifically, the group states that this construct has excellent potential in load-bearing cartilage applications, which is not supported by data from, for example, *in vivo* experiments. Regarding the drug release studies, the group showed that a laser-induced increase in temperature accelerated drug release. They suggested that controlling the laser power could aid in achieving controlled drug release. However, the authors state that drug release was upregulated with increasing temperatures (i.e., 42.7 °C and 45 °C), which might increase the risk of irreversible tissue damage upon long exposure times [112]. Furthermore, focusing a NIR laser on the printed construct *in vivo* would be a major challenge, since the penetration depth of NIR light is, on average, only 5 to 10 mm. This penetration depth can be increased to 30 mm using laser powers from 10 to 15 W, which also involves risks *in vivo* [113, 114].

Ceylan et al. conducted two-photon direct laser writing (DLW) to print a complex helical, hydrogel-based, enzymatically degradable microswimmer which is magnetically powered and controlled (Fig. 5). To increase the volume-to-surface ratio of the microswimmer, the group

chose a porous hydrogel network. This small change led to a higher capacity for therapeutics to be loaded and controllably released. The hydrogel formulation consisted of gelatin methacryloyl, lithium phenyl-(2,4,6-trimethylbenzoyl) phosphinate, and iron oxide nanoparticles coated with poly(ethylene glycol)amine. The addition of iron oxide nanoparticles, together with the geometry of the construct, facilitated movement of the microswimmer when exposed to a magnetic field. Iron oxide nanoparticles are FDA-approved [115] and a magnetic field is a safe way of controlling and powering microrobots, a very novel approach. However, as stated in the article, the helical shape of the construct needs a rotating magnetic field to power the microswimmer. Thus, a bulky MRI device is probably required to propel the microswimmers for applications in large *in vivo* models. Furthermore, the proposed constructs could only be loaded and printed correctly with a maximum nanoparticle concentration of 6 mg/mL, which might be too low for *in vivo* applications. To test drug release in certain conditions, the microswimmers were loaded with dextran-FITC, a drug-equivalent macromolecule. Interestingly, the elevated concentration of the disease marker enzyme, matrix metalloproteinase-2 (MMP-2), triggered the microswimmer

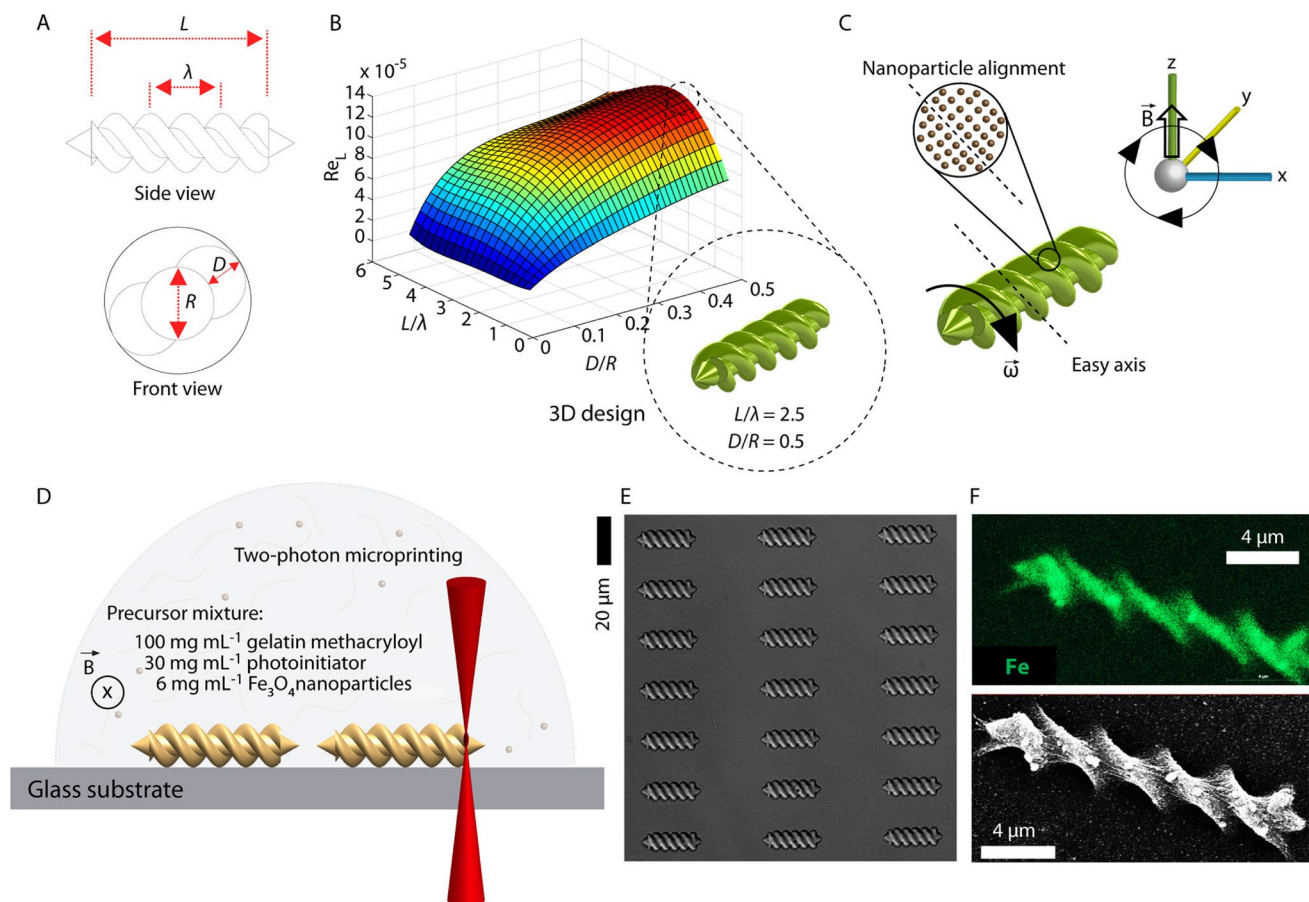


Fig. 5 Design and fabrication process of the 3D-printed hydrogel microswimmers presented by Ceylan et al. **a** Side view and front view of the microswimmer and definition of the parameters. **b** Computational simulation of fluid dynamics comparing the Reynolds number with respect to ratio of the L/λ and D/R ratio, to find maximum swimming velocity of the microswimmer. **c** Alignment of iron oxide nanoparticles which allows the construct to rotate under a rotating magnetic field. **d** Schematic representation of the fabrication process of microswimmers using DLW 3D printing. **e** Images of the construct and **f** X-ray spectroscopy mapping of nanoparticles showing that the particles were distributed homogeneously throughout the construct. Reproduced with permission from [116], Copyright 2019, ACS publications

to accelerate therapeutic cargo release. Here, the group shows a novel approach to releasing the model drug over time by making use of MMP-2 enzymes. This approach is extremely relevant, since a high concentration of MMP-2 is a common feature in different cancers. Another experiment in the paper demonstrated the release of anti-ErbB2 antibody-tagged magnetic nanoparticles from the microswimmers to target the SKBR3 breast cancer cell line. The paper emphasizes the importance of microswimmers and microrobots as potential theranostic devices in the field of regenerative medicine and targeted drug delivery. Nevertheless, optimization of the microswimmers to enhance the degree of freedom for complex tissue structures is something that the group is currently working towards [116].

4D-printed oral formulations

Melocchi et al. produced an impressive shape-memory expandable gastric retention drug-delivery system (SMX GRDDS). The group used the Kloner3D® 240 Twin (Kloner3D, I) equipped with a 0.5 mm nozzle to perform fused deposition modeling (FDM). The printed substance was a mixture of poly(vinyl alcohol) (PVA) and glycerol (GLY), with allopurinol (ALP), a xanthine oxidase inhibitor, as the model drug. The mixture was referred to as PVA05GLY-ALP, and a cylindrical helix-shaped structure with a diameter of 15 mm and height of 17 mm was printed with a speed of 23 mm/s. The group showed that they were able to print different shapes using printing molds. A capsule designed for oral intake was loaded with the SMX GRDDS

in its temporary shape. When the capsule was subjected to 0.1 M HCl at 37 °C, which simulates the acidic environment in the stomach, it began to degrade immediately and the printed construct was subjected to the 0.1 M HCl. Regarding drug release, the system showed a sustained release over the course of 2 h regardless of the printed shape. However, when a Eudragit® RS/Eudragit® RL coating was applied, the device released its content in a controlled manner over the span of 5 h. The group states that a long-lasting performance is desired for GRDDS. However, it should be noted that the authors did not show any results with other factors present in the stomach, like enzymes. Although the presented GRDDS is a novel 4D-printed device which showed good results, optimization will be necessary to further develop and test the system. In this respect, the group has already planned further studies [117].

4D-printed microneedles

Recently, Han et al. showed novel 4D printing of a microneedle array that enhanced tissue adhesion (Fig. 6). The group used a custom-built projection micro stereolithography (PμSL) to 3D-print a mixture of poly(ethylene glycol) diacrylate as a monomer, phenyl bis (2,4,6-trimethylbenzoyl) phosphine oxide as a photoinitiator, and Sudan I as a photo absorber. To enhance tissue adhesion for the microneedle array, Han et al. printed horizontally curved barbs on the microneedles that could deform into a curved geometry upon post-printing dissolving. The barbs resulted in skin adhesion that was increased 18-fold as compared to a needle without barbs; adhesion is regarded as important when a transdermal drug-eluting device is slowly releasing its drug over time. Transdermal drug delivery was demonstrated using the fluorescent Rhodamine B molecule as a model drug. Rhodamine B was loaded into the device by immersing the microneedles in a solution for 15 h, which might suggest that the loading of the microneedles should be optimized in future. The group performed experiments *in vitro*, using PBS, and *ex vivo* experiments on chicken breasts covered with cellophane that acted as a human skin model. They controlled the thickness and bending curvature of the barbs and, more importantly, the system demonstrated sustained drug release (i.e., 2.5 μg of Rhodamine B was released in 6 h) in the chicken breast skin-barrier model, indicating the potential of barbed-needle patches as a transdermal and *in vivo* drug delivery system. Thus, Han's group showed the first 4D-printed microneedles that could potentially be used for personalized transdermal drug delivery [118].

4D-printed drug-eluting implants

Many applications exist for stimuli-responsive implants for drug delivery [119–122]. Some groups have used novel 4D

printing techniques to create implants that could be used as drug delivery systems [123–129]. Only a few have incorporated a (model) drug inside a stimuli-responsive 3D-printed implant.

Earlier research conducted by Melocchi et al. demonstrated the feasibility of 4D printing an intravesical drug delivery system for bladder diseases based on PVA. Here, the group again used the Kloner3D® 240 Twin (Kloner3D, I) equipped with a 0.4 mm nozzle to perform FDM 3D printing with a tracer-containing formulation. The model drug used was caffeine (CFF), and the final tracer-containing formulation was referred to as PVA05GLY-CFF. PVA showed water-induced shape-memory behavior, which was regarded as the fourth dimension in this drug delivery system. The group showed production of I-, U-, and helix-shaped specimens and found that shape transformation was induced at 37 °C in aqueous media. The shape transformation also resulted in softening of the material, which could be beneficial *in vivo* to prevent damage to biological structures. *In vitro* experiments, using water at 37 °C, demonstrated a sustained drug release for 2 h. The group found that the drug release could be improved by choosing different polymers to fabricate the construct. Based on preliminary results, the study showed a biodegradable stimuli-responsive drug delivery system with controlled release of a model drug. Further studies should focus on cell experiments and, if possible, *in vivo* studies to further evaluate potential applications [117].

More recently, Salimi et al. produced a novel thermo-responsive supramolecular polyurethane (SPU) and used it as a matrix for drug-eluting implants. The group used a pneumatic-based extrusion bioprinter with a UV-LED curing system (CELLINK, Sweden) to print a bar-shaped implant from a mixture of SPU and poly(ethylene glycol) (PEG). Paracetamol (16 wt%) was incorporated in the bar-shaped implant as a model drug. The implant showed excellent biocompatibility and no significant cytotoxicity in mouse fibroblast cell line L929. The material itself was stiff yet flexible and offered a controlled release of paracetamol (i.e., 36 mg in 8.5 months, depending on the amount of PEG). Although the implant had some favorable features, Salimi et al. noticed deformation of the implant before and after drug release, which indicates that the transition temperatures of SPU should be optimized [130].

Future perspectives and conclusions

3D printing techniques have found a place in product development in biomedical and pharmaceutical arenas. These additive manufacturing methods offer fast and feasible production of formulations with complex geometries using computer software and computer-aided design. This approach helped in overcoming the need for multi-step

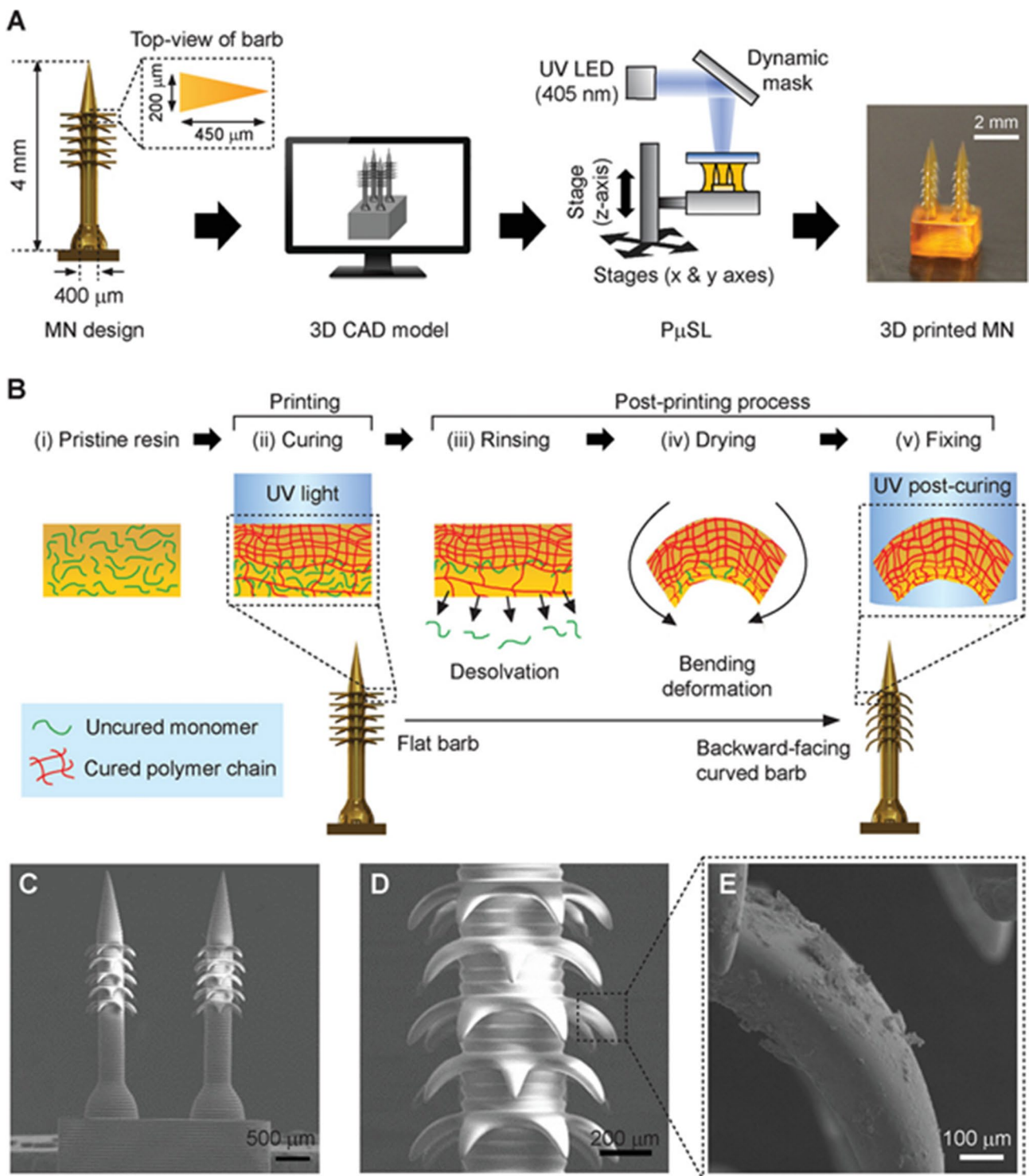


Fig. 6 4D printing of a bioinspired microneedle array by Han et al. **a** From the design towards 3D printing of the microneedles using PµSL. **b** Schematic illustration of the approach to realize 4D printing of barbs that could be deformed and fixed upon post-printing dissolv-

ing, bending, and UV curing. **c–e** Images from the SEM that depict the backward-facing barbs. Reproduced with permission from [118], Copyright 2020, John Wiley and Sons

and costly processes in the development and fabrication of several dosage forms. The first pharmaceutical product obtained from 3D bioprinting that was approved by the Food and Drug Administration was Spritam®, which reached the market in 2015. Several techniques, namely, inkjet printing, powder bed printing, selective laser sintering, pressure-assisted microsyringes, stereolithography, and fused deposition modelling, have been developed over the last twenty years. However, many of these techniques are still limited by a low-throughput compared to traditional medicine fabrication methods. Thus, scaling up is essential in bridging the gap towards commercialization of 3D-printed drug formulations. Other limitations of using 3D bioprinting within the pharmaceutical industry are set by the biomaterials themselves. High temperatures, which are regularly needed in 3D bioprinting or biomaterial sterilization methods, may not be ideal for the drug formulations within the biomaterial. We also foresee the use of new-generation (i.e., collagen-or fibrin-based) biomaterials, which show great biocompatibility and low immunogenicity, and may therefore aid in creating implantable drug delivery platforms [131, 132]. More recently, 4D printing has been introduced, and experiments have had significant economic and strategic outcomes in terms of scientific and technological developments. With the introduction of a fourth dimension—time—4D printing offers the capacity to transform virtual data into physical objects that mimic tissues, organs, and cells. Such smart materials are combined with 3D printing to record, store, and curate outputs in response to external stimuli. However, there is still a lot of room for progress within the field of 4D bioprinting. For example, for future widespread clinical applications, 4D-printed drug constructs must offer high sensitivity, high selectivity, and controlled release of drugs. Moreover, clinical safety, drug and biomaterial efficacy, and real-time control over the 4D stimuli response of the biomaterial need to be demonstrated. An interesting and novel trend that has potential in 4D bioprinting and which has not yet been used for pharmaceutical applications, is shape recovery hydrogels. These ‘smart’ biomaterials that can respond and change shape upon an external stimulus (e.g., temperature or pH) [133] can, ideally, be implanted at any site within the body by changing their shape, and can restore their function by recovering their original shape in vivo. The reversibility of 3D-printed materials allows for a two-way memory, or in other words, repetitive stimulation, which eradicates the need for reprogramming of the biomaterial [133]. In conclusion, 3D, and especially 4D, bioprinting open up a new paradigm within the drug delivery field, but there is still a long way to go for both to be regularly commercialized and implemented clinically.

Author contributions NW, MM, and DV contributed for the conceptualization, writing—original draft, literature review and visualization;

CS, JC, ES, and PS contributed for the revised version of the manuscript, for the editing, supervision and project administration.

Declarations

Conflict of interest The authors declare that there is no conflict of interest.

Ethical approval This article does not contain any studies with human or animal subjects performed by any of the authors.

References

- Ginsburg GS, Willard HF (2009) Genomic and personalized medicine: foundations and applications. *Transl Res J Lab Clin Med* 154:277–287. <https://doi.org/10.1016/j.trsl.2009.09.005>
- Terry SF (2015) Obama’s precision medicine initiative. *Genet Test Mol Biomarkers* 19:113–114. <https://doi.org/10.1089/gtmb.2015.1563>
- Abrahams E, Silver M (2009) The case for personalized medicine. *J Diabetes Sci Technol* 3:680–684. <https://doi.org/10.1177/193229680900300411>
- Goyanes A, Robles Martinez P, Buanz A et al (2015) Effect of geometry on drug release from 3D printed tablets. *Int J Pharm* 494:657–663. <https://doi.org/10.1016/j.ijpharm.2015.04.069>
- Piedade AP (2019) 4D printing: the shape-morphing in additive manufacturing. *J Funct Biomater* 10:9. <https://doi.org/10.3390/jfb10010009>
- Kim BS, Kwon YW, Kong JS et al (2018) 3D cell printing of in vitro stabilized skin model and in vivo pre-vascularized skin patch using tissue-specific extracellular matrix bioink: a step towards advanced skin tissue engineering. *Biomaterials* 168:38–53. <https://doi.org/10.1016/j.biomaterials.2018.03.040>
- Robles-Martinez P, Xu X, Trenfield SJ et al (2019) 3D printing of a multi-layered polypill containing six drugs using a novel stereolithographic method. *Pharmaceutics* 2019:11. <https://doi.org/10.3390/pharmaceutics11060274>
- West TG, Bradbury TJ (2019) 3D printing: a case of ZipDose® technology—world’s first 3D printing platform to obtain FDA approval for a pharmaceutical product. In: *3D and 4D printing in biomedical applications*, pp 53–79
- Murphy SV, Atala A (2014) 3D bioprinting of tissues and organs. *Nat Biotechnol* 32:773–785. <https://doi.org/10.1038/nbt.2958>
- Papaioannou TG, Manolesou D, Dimakakos E et al (2019) 3D bioprinting methods and techniques: applications on artificial blood vessel fabrication. *Acta Cardiol Sin* 35:284–289. [https://doi.org/10.6515/ACS.201905_35\(3\).20181115A](https://doi.org/10.6515/ACS.201905_35(3).20181115A)
- Ingber DE, Mow VC, Butler D et al (2006) Tissue engineering and developmental biology: going biomimetic. *Tissue Eng* 12:3265–3283. <https://doi.org/10.1089/ten.2006.12.3265>
- Teixeira AI, Nealey PF, Murphy CJ (2004) Responses of human keratocytes to micro- and nanostructured substrates. *J Biomed Mater Res Part A* 71:369–376. <https://doi.org/10.1002/jbm.a.30089>
- Derby B (2012) Printing and prototyping of tissues and scaffolds. *Science* 338:921. <https://doi.org/10.1126/science.1226340>
- An J, Chua CK, Mironov V (2016) A perspective on 4D bioprinting. *Int J Bioprint* 2:3. <https://doi.org/10.18063/ijb.2016.01.003>
- Gao B, Yang Q, Zhao X et al (2016) 4D bioprinting for biomedical applications. *Trends Biotechnol* 34:746–756. <https://doi.org/10.1016/j.tibtech.2016.03.004>

16. Gudapati H, Dey M, Ozbolat I (2016) A comprehensive review on droplet-based bioprinting: past, present and future. *Biomaterials* 102:20–42. <https://doi.org/10.1016/j.biomaterials.2016.06.012>
17. Hölzl K, Lin S, Tytgat L et al (2016) Bioink properties before, during and after 3D bioprinting. *Biofabrication* 8:032002. <https://doi.org/10.1088/1758-5090/8/3/032002>
18. Jeong H-J, Nam H, Jang J et al (2020) 3D bioprinting strategies for the regeneration of functional tubular tissues and organs. *Bioengineering* 2020:7. <https://doi.org/10.3390/bioengineering7020032>
19. Jia W, Gungor-Ozkerim PS, Zhang YS et al (2016) Direct 3D bioprinting of perfusable vascular constructs using a blend bioink. *Biomaterials* 106:58–68. <https://doi.org/10.1016/j.biomaterials.2016.07.038>
20. Graham AD, Olof SN, Burke MJ et al (2017) High-resolution patterned cellular constructs by droplet-based 3D printing. *Sci Rep* 7:7004. <https://doi.org/10.1038/s41598-017-06358-x>
21. de Grujil FR, van Kranen HJ, Mullenders LHF (2001) UV-induced DNA damage, repair, mutations and oncogenic pathways in skin cancer. *J Photochem Photobiol B* 63:19–27. [https://doi.org/10.1016/S1011-1344\(01\)00199-3](https://doi.org/10.1016/S1011-1344(01)00199-3)
22. Kang H-W, Lee SJ, Ko IK et al (2016) A 3D bioprinting system to produce human-scale tissue constructs with structural integrity. *Nat Biotechnol* 34:312–319. <https://doi.org/10.1038/nbt.3413>
23. Wu W, DeConinck A, Lewis JA (2011) Omnidirectional printing of 3D microvascular networks. *Adv Mater* 23:H178–H183. <https://doi.org/10.1002/adma.201004625>
24. Hribar KC, Soman P, Warner J et al (2014) Light-assisted direct-write of 3D functional biomaterials. *Lab Chip* 14:268–275. <https://doi.org/10.1039/C3LC50634G>
25. Zhang AP, Qu X, Soman P et al (2012) Rapid fabrication of complex 3D extracellular microenvironments by dynamic optical projection stereolithography. *Adv Mater* 24:4266–4270. <https://doi.org/10.1002/adma.201202024>
26. Tumbleston JR, Shirvanyants D, Ermoshkin N et al (2015) Continuous liquid interface production of 3D objects. *Science* 347:1349. <https://doi.org/10.1126/science.aaa2397>
27. Grigoryan B, Sazer DW, Avila A et al (2021) Development, characterization, and applications of multi-material stereolithography bioprinting. *Sci Rep* 11:3171. <https://doi.org/10.1038/s41598-021-82102-w>
28. Awad A, Fina F, Goyanes A et al (2020) 3D printing: principles and pharmaceutical applications of selective laser sintering. *Int J Pharm* 586:119594. <https://doi.org/10.1016/j.ijpharm.2020.119594>
29. Kulinowski P, Malczewski P, Pesta E et al (2021) Selective laser sintering (SLS) technique for pharmaceutical applications—development of high dose controlled release printlets. *Addit Manuf* 38:101761. <https://doi.org/10.1016/j.addma.2020.101761>
30. Melchels FPW, Feijen J, Grijpma DW (2010) A review on stereolithography and its applications in biomedical engineering. *Biomaterials* 31:6121–6130. <https://doi.org/10.1016/j.biomaterials.2010.04.050>
31. Wüst S, Müller R, Hofmann S (2011) Controlled positioning of cells in biomaterials—approaches towards 3D tissue printing. *J Funct Biomater* 2011:2. <https://doi.org/10.3390/jfb2030119>
32. Tetsuka H, Shin SR (2020) Materials and technical innovations in 3D printing in biomedical applications. *J Mater Chem B* 8:2930–2950. <https://doi.org/10.1039/D0TB00034E>
33. Li X, Liu B, Pei B et al (2020) Inkjet bioprinting of biomaterials. *Chem Rev* 120:10793–10833. <https://doi.org/10.1021/acs.chemrev.0c00008>
34. Li J, Chen M, Fan X et al (2016) Recent advances in bioprinting techniques: approaches, applications and future prospects. *J Transl Med* 14:271. <https://doi.org/10.1186/s12967-016-1028-0>
35. Zein I, Huttmacher DW, Tan KC et al (2002) Fused deposition modeling of novel scaffold architectures for tissue engineering applications. *Biomaterials* 23:1169–1185. [https://doi.org/10.1016/s0142-9612\(01\)00232-0](https://doi.org/10.1016/s0142-9612(01)00232-0)
36. Wang Z, Kumar H, Tian Z et al (2018) Visible light photoinitiation of cell-adhesive gelatin methacryloyl hydrogels for stereolithography 3D bioprinting. *ACS Appl Mater Interfaces* 10:26859–26869. <https://doi.org/10.1021/acsami.8b06607>
37. Catros S, Fricain JC, Guillotin B et al (2011) Laser-assisted bioprinting for creating on-demand patterns of human osteoprogenitor cells and nano-hydroxyapatite. *Biofabrication* 3:025001. <https://doi.org/10.1088/1758-5082/3/2/025001>
38. Baker AB, Bates SRG, Llewellyn-Jones TM et al (2019) 4D printing with robust thermoplastic polyurethane hydrogel-elastomer trilayers. *Mater Des* 163:107544. <https://doi.org/10.1016/j.matdes.2018.107544>
39. Odent J, Vanderstappen S, Toncheva A et al (2019) Hierarchical chemomechanical encoding of multi-responsive hydrogel actuators via 3D printing. *J Mater Chem A* 7:15395–15403. <https://doi.org/10.1039/C9TA03547H>
40. Hu Y, Wang Z, Jin D et al (2020) Botanical-inspired 4D printing of hydrogel at the microscale. *Adv Funct Mater* 30:1907377. <https://doi.org/10.1002/adfm.201907377>
41. Bakarich SE, Gorkin R III, Panhuis MIH et al (2015) 4D printing with mechanically robust, thermally actuating hydrogels. *Macromol Rapid Commun* 2015(36):1211–1217. <https://doi.org/10.1002/marc.201500079>
42. Seo JW, Shin SR, Park YJ et al (2020) Hydrogel production platform with dynamic movement using photo-crosslinkable/temperature reversible chitosan polymer and stereolithography 4D printing technology. *Tissue Eng Regen Med* 17:423–431. <https://doi.org/10.1007/s13770-020-00264-6>
43. Wan Z, Zhang P, Liu Y et al (2020) Four-dimensional bioprinting: current developments and applications in bone tissue engineering. *Acta Biomater* 101:26–42. <https://doi.org/10.1016/j.actbio.2019.10.038>
44. Ashammakhi N, Ahadian S, Zengjie F et al (2018) Advances and future perspectives in 4D bioprinting. *Biotechnol J* 13:e1800148. <https://doi.org/10.1002/biot.201800148>
45. Morsink MAJ, Willems NGA, Leijten J et al (2020) Immune organs and immune cells on a chip: an overview of biomedical applications. *Micromachines* 11:849
46. Elkhoury K, Morsink M, Sanchez-Gonzalez L et al (2021) Biofabrication of natural hydrogels for cardiac, neural, and bone tissue engineering applications. *Bioactive Mater* 6:3904–3923. <https://doi.org/10.1016/j.bioactmat.2021.03.040>
47. Gungor-Ozkerim PS, Inci I, Zhang YS et al (2018) Bioinks for 3D bioprinting: an overview. *Biomater Sci* 6:915–946. <https://doi.org/10.1039/C7BM00765E>
48. Zhang YS, Yue K, Aleman J et al (2017) 3D bioprinting for tissue and organ fabrication. *Ann Biomed Eng* 45:148–163. <https://doi.org/10.1007/s10439-016-1612-8>
49. Faramarzi N, Yazdi IK, Nabavinia M et al (2018) Patient-specific bioinks for 3D bioprinting of tissue engineering scaffolds. *Adv Healthcare Mater* 7:1701347. <https://doi.org/10.1002/adhm.201701347>
50. Dababneh AB, Ozbolat IT (2014) Bioprinting technology: a current state-of-the-art review. *J Manuf Sci Eng* 2014:136. <https://doi.org/10.1115/1.4028512>
51. Henry S, McAllister DV, Allen MG et al (1998) Microfabricated microneedles: a novel approach to transdermal drug delivery. *J Pharm Sci* 87:922–925. <https://doi.org/10.1021/js980042+>

52. Moussi K, Bukhamsin A, Hidalgo T et al (2020) Biocompatible 3D printed microneedles for transdermal, intradermal, and percutaneous applications. *Adv Eng Mater* 22:1901358. <https://doi.org/10.1002/adem.201901358>
53. Moussi K, Kosel J (2018) 3-D printed biocompatible microbellows membranes. *J Microelectromech Syst* 27:472–478. <https://doi.org/10.1109/JMEMS.2018.2819994>
54. Ross S, Scoutaris N, Lamprou D et al (2015) Inkjet printing of insulin microneedles for transdermal delivery. *Drug Deliv Transl Res* 5:451–461. <https://doi.org/10.1007/s13346-015-0251-1>
55. Uddin MJ, Scoutaris N, Klepetsanis P et al (2015) Inkjet printing of transdermal microneedles for the delivery of anticancer agents. *Int J Pharm* 494:593–602. <https://doi.org/10.1016/j.ijpharm.2015.01.038>
56. Yin M, Xiao L, Liu Q et al (2019) 3D Printed microheater sensor-integrated, drug-encapsulated microneedle patch system for pain management. *Adv Healthcare Mater* 8:1901170. <https://doi.org/10.1002/adhm.201901170>
57. Park J-H, Lee J-W, Kim Y-C et al (2008) The effect of heat on skin permeability. *Int J Pharm* 359:94–103. <https://doi.org/10.1016/j.ijpharm.2008.03.032>
58. Pere CPP, Economidou SN, Lall G et al (2018) 3D printed microneedles for insulin skin delivery. *Int J Pharm* 544:425–432. <https://doi.org/10.1016/j.ijpharm.2018.03.031>
59. Luzuriaga MA, Berry DR, Reagan JC et al (2018) Biodegradable 3D printed polymer microneedles for transdermal drug delivery. *Lab Chip* 18:1223–1230. <https://doi.org/10.1039/C8LC00098K>
60. Khaled SA, Burley JC, Alexander MR et al (2015) 3D printing of five-in-one dose combination polypill with defined immediate and sustained release profiles. *J Control Release* 217:308–314. <https://doi.org/10.1016/j.jconrel.2015.09.028>
61. Mathew E, Domínguez-Robles J, Stewart SA et al (2019) Fused deposition modeling as an effective tool for anti-infective dialysis catheter fabrication. *ACS Biomater Sci Eng* 5:6300–6310. <https://doi.org/10.1021/acsbomaterials.9b01185>
62. Khan W, Farah S, Domb AJ (2012) Drug eluting stents: developments and current status. *J Control Release Soc* 161:703–712. <https://doi.org/10.1016/j.jconrel.2012.02.010>
63. Seol Y-J, Lee H, Copus JS et al (2018) 3D bioprinted biomask for facial skin reconstruction. *Bioprinting* 10:e00028. <https://doi.org/10.1016/j.bprint.2018.e00028>
64. Augustine R (2018) Skin bioprinting: a novel approach for creating artificial skin from synthetic and natural building blocks. *Prog Biomater* 7:77–92. <https://doi.org/10.1007/s40204-018-0087-0>
65. Si H, Xing T, Ding Y et al (2019) 3D bioprinting of the sustained drug release wound dressing with double-crosslinked hyaluronic-acid-based hydrogels. *Polymers* 2019:11. <https://doi.org/10.3390/polym11101584>
66. Long J, Etxeberria AE, Nand AV et al (2019) A 3D printed chitosan-pectin hydrogel wound dressing for lidocaine hydrochloride delivery. *Mater Sci Eng C* 104:109873. <https://doi.org/10.1016/j.msec.2019.109873>
67. Wang S, Xiong Y, Chen J et al (2019) Three dimensional printing bilayer membrane scaffold promotes wound healing. *Front Bioeng Biotechnol* 7:348. <https://doi.org/10.3389/fbioe.2019.00348>
68. Maver T, Smrke DM, Kurečić M et al (2018) Combining 3D printing and electrospinning for preparation of pain-relieving wound-dressing materials. *J Sol-Gel Sci Technol* 88:33–48. <https://doi.org/10.1007/s10971-018-4630-1>
69. Muwaffak Z, Goyanes A, Clark V et al (2017) Patient-specific 3D scanned and 3D printed antimicrobial polycaprolactone wound dressings. *Int J Pharm* 527:161–170. <https://doi.org/10.1016/j.ijpharm.2017.04.077>
70. Souto EB, Campos JC, Filho SC et al (2019) 3D printing in the design of pharmaceutical dosage forms. *Pharm Dev Technol* 24:1044–1053. <https://doi.org/10.1080/10837450.2019.1630426>
71. Rowe CW, Katstra WE, Palazzolo RD et al (2000) Multimechanism oral dosage forms fabricated by three dimensional printing. *J Control Release Off J Control Release Soc* 66:11–17. [https://doi.org/10.1016/s0168-3659\(99\)00224-2](https://doi.org/10.1016/s0168-3659(99)00224-2)
72. Sadia M, Arafat B, Ahmed W et al (2018) Channelled tablets: an innovative approach to accelerating drug release from 3D printed tablets. *J Control Release* 269:355–363. <https://doi.org/10.1016/j.jconrel.2017.11.022>
73. Khaled SA, Alexander MR, Wildman RD et al (2018) 3D extrusion printing of high drug loading immediate release paracetamol tablets. *Int J Pharm* 538:223–230. <https://doi.org/10.1016/j.ijpharm.2018.01.024>
74. Li Q, Wen H, Jia D et al (2017) Preparation and investigation of controlled-release glipizide novel oral device with three-dimensional printing. *Int J Pharm* 525:5–11. <https://doi.org/10.1016/j.ijpharm.2017.03.066>
75. Kadry H, Al-Hilal TA, Keshavarz A et al (2018) Multi-purposable filaments of HPMC for 3D printing of medications with tailored drug release and timed-absorption. *Int J Pharm* 544:285–296. <https://doi.org/10.1016/j.ijpharm.2018.04.010>
76. Li Q, Guan X, Cui M et al (2018) Preparation and investigation of novel gastro-floating tablets with 3D extrusion-based printing. *Int J Pharm* 535:325–332. <https://doi.org/10.1016/j.ijpharm.2017.10.037>
77. Linares V, Casas M, Caraballo I (2019) Printfills: 3D printed systems combining fused deposition modeling and injection volume filling. Application to colon-specific drug delivery. *Eur J Pharm Biopharm* 2019(134):138–143. <https://doi.org/10.1016/j.ejpb.2018.11.021>
78. Liang K, Carmone S, Brambilla D et al (2018) 3D printing of a wearable personalized oral delivery device: a first-in-human study. *Sci Adv* 4:eaat2544. <https://doi.org/10.1126/sciadv.aat2544>
79. Wang Y, Miao Y, Zhang J et al (2018) Three-dimensional printing of shape memory hydrogels with internal structure for drug delivery. *Mater Sci Eng C* 84:44–51. <https://doi.org/10.1016/j.msec.2017.11.025>
80. Kabb CP, O'Bryan CS, Deng CC et al (2018) Photoreversible covalent hydrogels for soft-matter additive manufacturing. *ACS Appl Mater Interf* 10:16793–16801. <https://doi.org/10.1021/acsaami.8b02441>
81. Wang Y, Sun L, Mei Z et al (2020) 3D printed biodegradable implants as an individualized drug delivery system for local chemotherapy of osteosarcoma. *Mater Des* 186:108336. <https://doi.org/10.1016/j.matdes.2019.108336>
82. Yang Y, Qiao X, Huang R et al (2020) E-jet 3D printed drug delivery implants to inhibit growth and metastasis of orthotopic breast cancer. *Biomaterials* 230:119618. <https://doi.org/10.1016/j.biomaterials.2019.119618>
83. Maheshwari RK, Singh AK, Gaddipati J et al (2006) Multiple biological activities of curcumin: a short review. *Life Sci* 78:2081–2087. <https://doi.org/10.1016/j.lfs.2005.12.007>
84. Bose S, Sarkar N, Banerjee D (2018) Effects of PCL, PEG and PLGA polymers on curcumin release from calcium phosphate matrix for in vitro and in vivo bone regeneration. *Mater Today Chem* 8:110–120. <https://doi.org/10.1016/j.mtchem.2018.03.005>
85. Dydak K, Junka A, Szymczyk P et al (2018) Development and biological evaluation of Ti6Al7Nb scaffold implants coated with gentamycin-saturated bacterial cellulose biomaterial. *PLoS ONE* 13:e0205205. <https://doi.org/10.1371/journal.pone.0205205>
86. Hosseinzadeh R, Mirani B, Pagan E et al (2019) A drug-eluting 3D-printed mesh (GlioMesh) for management of glioblastoma. *Adv Ther* 2:1900113. <https://doi.org/10.1002/adtp.201900113>
87. Weisman JA, Ballard DH, Jammalamadaka U et al (2019) 3D printed antibiotic and chemotherapeutic eluting catheters for potential use in interventional radiology: in vitro proof of concept

- study. *Acad Radiol* 26:270–274. <https://doi.org/10.1016/j.acra.2018.03.022>
88. Nomi M, Atala A, Coppi PD et al (2002) Principals of neovascularization for tissue engineering. *Mol Aspects Med* 23:463–483. [https://doi.org/10.1016/S0098-2997\(02\)00008-0](https://doi.org/10.1016/S0098-2997(02)00008-0)
 89. Benjamin S, Sheyn D, Ben-David S et al (2012) Oxygenated environment enhances both stem cell survival and osteogenic differentiation. *Tissue Eng Part A* 19:748–758. <https://doi.org/10.1089/ten.tea.2012.0298>
 90. Lu Z, Jiang X, Chen M et al (2019) An oxygen-releasing device to improve the survival of mesenchymal stem cells in tissue engineering. *Biofabrication* 11:045012. <https://doi.org/10.1088/1758-5090/ab332a>
 91. Touri M, Moztarzadeh F, Osman NAA et al (2019) Optimisation and biological activities of bioceramic robocast scaffolds provided with an oxygen-releasing coating for bone tissue engineering applications. *Ceram Int* 45:805–816. <https://doi.org/10.1016/j.ceramint.2018.09.247>
 92. Touri M, Moztarzadeh F, Osman NAA et al (2018) 3D-printed biphasic calcium phosphate scaffolds coated with an oxygen generating system for enhancing engineered tissue survival. *Mater Sci Eng C* 84:236–242. <https://doi.org/10.1016/j.msec.2017.11.037>
 93. Kondiah PJ, Kondiah PPD, Choonara YE et al (2020) A 3D bioprinted pseudo-bone drug delivery scaffold for bone tissue engineering. *Pharmaceutics* 2020:12. <https://doi.org/10.3390/pharmaceutics12020166>
 94. Sharma R, Smits IPM, De La Vega L et al (2020) 3D bioprinting pluripotent stem cell derived neural tissues using a novel fibrin bioink containing drug releasing microspheres. *Front Bioeng Biotechnol* 8:57
 95. Byambaa B, Annabi N, Yue K et al (2017) Bioprinted osteogenic and vasculogenic patterns for engineering 3D bone tissue. *Adv Healthcare Mater* 6:1700015. <https://doi.org/10.1002/adhm.201700015>
 96. Chen S, Shi Y, Zhang X et al (2020) Evaluation of BMP-2 and VEGF loaded 3D printed hydroxyapatite composite scaffolds with enhanced osteogenic capacity in vitro and in vivo. *Mater Sci Eng C* 112:110893. <https://doi.org/10.1016/j.msec.2020.110893>
 97. Poldervaart MT, Gremmels H, van Deventer K et al (2014) Prolonged presence of VEGF promotes vascularization in 3D bioprinted scaffolds with defined architecture. *J Control Release* 184:58–66. <https://doi.org/10.1016/j.jconrel.2014.04.007>
 98. Kim B-S, Yang S-S, Kim CS (2018) Incorporation of BMP-2 nanoparticles on the surface of a 3D-printed hydroxyapatite scaffold using an ϵ -polycaprolactone polymer emulsion coating method for bone tissue engineering. *Colloids Surf B* 170:421–429. <https://doi.org/10.1016/j.colsurfb.2018.06.043>
 99. Fu J, Yu X, Jin Y (2018) 3D printing of vaginal rings with personalized shapes for controlled release of progesterone. *Int J Pharm* 539:75–82. <https://doi.org/10.1016/j.ijpharm.2018.01.036>
 100. Martinez PR, Goyanes A, Basit AW et al (2018) Influence of geometry on the drug release profiles of stereolithographic (SLA) 3D-printed tablets. *AAPS PharmSciTech* 19:3355–3361. <https://doi.org/10.1208/s12249-018-1075-3>
 101. Lim SH, Ng JY, Kang L (2017) Three-dimensional printing of a microneedle array on personalized curved surfaces for dual-pronged treatment of trigger finger. *Biofabrication* 9:015010. <https://doi.org/10.1088/1758-5090/9/1/015010>
 102. Sun Y, Soh S (2015) Printing tablets with fully customizable release profiles for personalized medicine. *Adv Mater* 27:7847–7853. <https://doi.org/10.1002/adma.201504122>
 103. Tan YJN, Yong WP, Kochhar JS et al (2020) On-demand fully customizable drug tablets via 3D printing technology for personalized medicine. *J Control Release* 322:42–52. <https://doi.org/10.1016/j.jconrel.2020.02.046>
 104. Goyanes A, Det-Amornrat U, Wang J et al (2016) 3D scanning and 3D printing as innovative technologies for fabricating personalized topical drug delivery systems. *J Control Release* 234:41–48. <https://doi.org/10.1016/j.jconrel.2016.05.034>
 105. Scoutaris N, Ross SA, Douroumis D (2018) 3D printed “starmix” drug loaded dosage forms for paediatric applications. *Pharm Res* 35:34. <https://doi.org/10.1007/s11095-017-2284-2>
 106. Preis M, Breikreutz J, Sandler N (2015) Perspective: concepts of printing technologies for oral film formulations. *Int J Pharm* 494:578–584. <https://doi.org/10.1016/j.ijpharm.2015.02.032>
 107. Clark EA, Alexander MR, Irvine DJ et al (2017) 3D printing of tablets using inkjet with UV photoinitiation. *Int J Pharm* 529:523–530. <https://doi.org/10.1016/j.ijpharm.2017.06.085>
 108. Tagami T, Fukushige K, Ogawa E et al (2017) 3D printing factors important for the fabrication of polyvinylalcohol filament-based tablets. *Biol Pharm Bull* 40:357–364. <https://doi.org/10.1248/bpb.b16-00878>
 109. Mukhopadhyay P, Sarkar K, Bhattacharya S et al (2014) pH sensitive N-succinyl chitosan grafted polyacrylamide hydrogel for oral insulin delivery. *Carbohydr Polym* 112:627–637. <https://doi.org/10.1016/j.carbpol.2014.06.045>
 110. Larush L, Kaner I, Fluksman A et al (2017) 3D printing of responsive hydrogels for drug-delivery systems. *J 3D Print Med* 1:219–229. <https://doi.org/10.2217/3dp-2017-0009>
 111. Dai W, Guo H, Gao B et al (2019) Double network shape memory hydrogels activated by near-infrared with high mechanical toughness, nontoxicity, and 3D printability. *Chem Eng J* 356:934–949. <https://doi.org/10.1016/j.cej.2018.09.078>
 112. Wood BJ, Ramkaransingh JR, Fojo T et al (2002) Percutaneous tumor ablation with radiofrequency. *Cancer* 94:443–451. <https://doi.org/10.1002/cncr.10234>
 113. Jiang Y, Yang Y, Zheng X et al (2020) Multifunctional load-bearing hybrid hydrogel with combined drug release and photothermal conversion functions. *NPG Asia Mater* 12:18. <https://doi.org/10.1038/s41427-020-0199-6>
 114. Henderson TA, Morries LD (2015) Near-infrared photonic energy penetration: can infrared phototherapy effectively reach the human brain? *Neuropsychiatr Dis Treat* 11:2191–2208. <https://doi.org/10.2147/NDT.S78182>
 115. Abo-Zeid Y, Ismail NSM, McLean GR et al (2020) A molecular docking study repurposes FDA approved iron oxide nanoparticles to treat and control COVID-19 infection. *Eur J Pharm Sci* 153:105465. <https://doi.org/10.1016/j.ejps.2020.105465>
 116. Ceylan H, Yasa IC, Yasa O et al (2019) 3D-printed biodegradable microswimmer for theranostic cargo delivery and release. *ACS Nano* 13:3353–3362. <https://doi.org/10.1021/acsnano.8b09233>
 117. Melocchi A, Ubaldi M, Inverardi N et al (2019) Expandable drug delivery system for gastric retention based on shape memory polymers: development via 4D printing and extrusion. *Int J Pharm* 571:118700. <https://doi.org/10.1016/j.ijpharm.2019.118700>
 118. Han D, Morde RS, Mariani S et al (2020) 4D printing of a bioinspired microneedle array with backward-facing barbs for enhanced tissue adhesion. *Adv Funct Mater* 30:1909197. <https://doi.org/10.1002/adfm.201909197>
 119. Liu X, Zhao K, Gong T et al (2014) Delivery of growth factors using a smart porous nanocomposite scaffold to repair a mandibular bone defect. *Biomacromol* 15:1019–1030. <https://doi.org/10.1021/bm401911p>
 120. Zhao X, Dong R, Guo B et al (2017) Dopamine-incorporated dual bioactive electroactive shape memory polyurethane elastomers with physiological shape recovery temperature, high stretchability, and enhanced C2C12 myogenic differentiation. *ACS Appl Mater Interf* 9:29595–29611. <https://doi.org/10.1021/acsami.7b10583>

121. Mikkonen J, Uurto I, Isotalo T et al (2009) Drug-eluting bioabsorbable stents—an in vitro study. *Acta Biomater* 5:2894–2900. <https://doi.org/10.1016/j.actbio.2009.03.039>
122. Uurto I, Mikkonen J, Parkkinen J et al (2005) Drug-eluting biodegradable poly-D/L-lactic acid vascular stents: an experimental pilot study. *J Endovasc Ther* 12:371–379. <https://doi.org/10.1583/05-1525.1>
123. Song Z, Ren L, Zhao C et al (2020) Biomimetic nonuniform, dual-stimuli self-morphing enabled by gradient four-dimensional printing. *ACS Appl Mater Interf* 12:6351–6361. <https://doi.org/10.1021/acsami.9b17577>
124. Zhang F, Wang L, Zheng Z et al (2019) Magnetic programming of 4D printed shape memory composite structures. *Compos A Appl Sci Manuf* 125:105571. <https://doi.org/10.1016/j.compositesa.2019.105571>
125. Jia H, Gu S-Y, Chang K (2018) 3D printed self-expandable vascular stents from biodegradable shape memory polymer. *Adv Polym Technol* 37:3222–3228. <https://doi.org/10.1002/adv.22091>
126. Kashyap D, Kishore Kumar P, Kanagaraj S (2018) 4D printed porous radiopaque shape memory polyurethane for endovascular embolization. *Addit Manuf* 24:687–695. <https://doi.org/10.1016/j.addma.2018.04.009>
127. Pandey A, Singh G, Singh S et al (2020) 3D printed biodegradable functional temperature-stimuli shape memory polymer for customized scaffoldings. *J Mech Behav Biomed Mater* 108:103781. <https://doi.org/10.1016/j.jmbbm.2020.103781>
128. Guo Y, Belgodere JA, Ma Y et al (2019) Directed printing and reconfiguration of thermoresponsive silica-pNIPAM nanocomposites. *Macromol Rapid Commun* 40:1900191. <https://doi.org/10.1002/marc.201900191>
129. Igor S, Vladimir S (2018) 4D manufacturing of intermetallic SMA fabricated by SLM process. In: *Proceedings of the Proc.SPIE*
130. Salimi S, Wu Y, Barreiros MIE et al (2020) A 3D printed drug delivery implant formed from a dynamic supramolecular polyurethane formulation. *Polym Chem* 11:3453–3464. <https://doi.org/10.1039/D0PY00068J>
131. Osidak EO, Kozhukhov VI, Osidak MS et al (2020) Collagen as bioink for bioprinting: a comprehensive review. *Int J Bioprint* 6:270. <https://doi.org/10.18063/ijb.v6i3.270>
132. Shpichka A, Osipova D, Efremov Y et al (2020) Fibrin-based bioinks: new tricks from an old dog. *Int J Bioprint* 6:269. <https://doi.org/10.18063/ijb.v6i3.269>
133. Lee AY, An J, Chua CK et al (2019) Preliminary investigation of the reversible 4D printing of a dual-layer component. *Engineering* 5:1159–1170. <https://doi.org/10.1016/j.eng.2019.09.007>